Academia Journal of Environmetal Science 7(3): 009-029, March 2019
DOI: 10.15413/ajes.2019.0104
ISSN: ISSN 2315-778X

Academia Publishing

Research Paper

Morphometric characteristics of alluvial fans in Southern Turkey: implications for fault activity in the Anatolia, Arabia, Africa Triple Junction Region

Atilla Karataş[1]* and Sarah J. Boulton[2]

[1]Marmara University, Geography Department, 34722İstanbul, Turkey.
[2]Centre for Research in Earth Sciences, School of Geography, Earth and Environmental Sciences, Plymouth University, Plymouth, Devon PL4 8AA, UK.

Corresponding author. E-mail: atilla.karatas@marmara.edu.tr. Tel.: +905333661735.

Accepted 28th March, 2019

ABSTRACT

Although, there are numerous studies investigating the boundary between the Anatolian, African and Arabian plates, there are still no definitive results on this topic. Continuing intense tectonic deformation in the area has caused tectonic lines composed of various types of faults to interact and it is necessary to accurately identify the plate borders in the convergence area which is globally and regionally important. Therefore, the impact of tectonic deformation on the current alluvial fans was measured through morphometric analysis methods such as concavity index, best fitted ellipse and sinuosity index to define the relationship between fault lines by presenting their recent behavior and the findings were evaluated in the light of kinematic-geodetic data. Thus, the relationship between tectonic belts which reflect similar effects had been considered at length by trying to describe the deformation effect of current tectonics on alluvial fans. Results showed that Dead Sea Fault Zone - the border of Arabian-African plates- and Cyprus Arc (CA) -the northern border of Africa- intersect on the north of Amik Plain and that East Anatolian Fault Zone –the south border of Anatolia- was moved further away from this intersection point to Türkoğlu since Late Miocene by Arabia's motions to the North. Continuation of this fault in the west of Türkoğlu intersected Amanos Mountains with many branches in northeastern-southwestern direction and created a plate border shaped by faults from north to south with decreased tectonic activities.

Key words: Alluvial fan morphometry, East Anatolian Fault, Maraş/Türkoğlu/Amik Triple Junction, globaltectonics.

INTRODUCTION

Morphometry, the measurement and mathematical analysis of landscape relief characteristics related to shape and dimension (Horton, 1945; Strahler, 1952; Mahadevaswamy et al., 2011) has been used in geomorphological studies since the middle of the last century as a result of efforts to objectively define and quantify relief by removing subjective descriptions (Heimann and Ron, 1993). Pioneering analytical studies in geomorphology undertaken by researchers such as Horton (1932, 1945), Strahler (1952, 1957), Schumm (1956), Leopold and Miller (1956), Melton (1957), Hack (1957) and Morisawa (1959) matured with the help of second generation studies led by Strahler (1964), Eagleson (1970), Doornkamp and Cuchlaine (1971) and Hack (1973). More recently, the use of remote sensing has become popular in morphometric analyses and landscapes can now be quickly and cheaply investigated using widely available digital datasets (Krishnamurthy et al., 1996; Nag, 1998; Nag and Chakraborthy, 2003; Gürsoy et al., 2011).

Alluvial fans have been the topic of these morphometric analyses and have been examined from a number of aspects; for example, fan geometry (Bull, 1961, 1964; Lecce, 1990), surface geomorphology (Denny, 1965; Stock et al., 2008), fluvial geomorphology (Blair and McPherson, 1994;

Calvache et al., 1997) and hydrogeomorphic structure (Marchi et al., 2010). As a result, various measurement techniques were developed for the classification and categorization of alluvial fans and new methods continue to evolve (Bull, 1962; Denny, 1967; Beaumont, 1972; Hooke and Roher, 1979; Harvey, 1987; Marchi et al., 1993; Mills, 2000). These methods allow the differentiation of factors that cause changes in the forms of topographic units such as alluvial fans (Oguchi and Oguchi, 2004: 128). Although fan sequences mostly respond to climatic controls, tectonic setting is the main parameter in controlling the location and setting of mountain front fans (Harvey et al., 2005). Alluvial fans are mainly observed in areas where basin-range morphology is dominant (Bull, 1977; Erinç, 2000; Burbank and Anderson, 2001; Goudie, 2004; Hoşgören, 2011) creating suitable environments with which to detect neo-tectonic traces; primarily the fault morphology (Tatar et al., 2004).

In this context, some features of alluvial fans such as morphometric characteristics (Bahrami, 2013), curved radial profiles (Bull, 1964), vertical sediment accumulation (Calvache et al., 1997), channel incision rates on alluvial fans (Lee et al., 2001) and tilting direction and degree (Pinter and Keller, 1995a) have been correlated to active faulting. This is due to alluvial fans acting as recorders of tectonics through their structure and sediment architecture. Fans located on active lineaments may develop surface fault traces after movements on fault or faults, as well as, anomalies in the sediment stratigraphy (Wells and Harvey, 1987; Blair and McPherson, 1994). Therefore, the investigation and interpretation of sedimentological, structural and geomorphic features can reveal much about the active faulting shaping of the landforms.

The aim of this research is to investigate the active tectonic structures of southern Turkey using a range of morphometric parameters derived from active and relict alluvial fans present in the study area. Topographic metrics will give insight into the sedimentological and climatic processes shaping the fans but also the underlying tectonic controls.

Geological background

The northward migration of the African plate towards the Eurasian plate during late Eocene-early Miocene period resulted in the formation of a north-dipping subduction zone bordering southern Anatolia (Şengör and Yılmaz, 1983). Following the complete closure of the Southern Branch of the Neo-Tethys in the region during the middle-late Miocene, the Eurasian-Arabian collision along the Bitlis-Zagros Suture Zone (BZSZ) produced north-south directed shortening, this strain was most pronounced in Eastern Anatolia (Şengör and Yılmaz, 1983: 53). However, thickening of continental crust also caused increased resistance against north-south oriented compression resulting in the westwards extrusion of Anatolia towards the Aegean and central Mediterranean (McKenzie, 1972; Yılmaz et al., 1985; Reilinger et al., 1997). The westwards motion of the Anatolia microplate was accommodated through the formation of the North (NAFZ) and East Anatolian Fault Zones (EAFZ) (Şengör, 1979) during the late Miocene to early Pliocene. Furthermore, the differential northwards movement of the Arabian plate compared to African plate resulted in the development of the Dead Sea Fault Zone (DSFZ) (Quennell, 1956; Freund, 1965; Garfunkel, 1981; Garfunkel et al., 1981; Courtillot et al., 1987; Joffe and Garfunkel, 1987; Brink et al., 1999) during the middle Miocene (Lyberis, 1988; Garfunkel and Ben-Avraham, 1996). The DSFZ subsequently propagated northwards reaching the Amik Plain during the Pliocene. However, the diffuse and complex nature of this continental plate boundary led to debate within the scientific literature on the precise location of plate margins, this is especially true in the easternmost Mediterranean, where the location of the triple junction between the DSFZ, EAFZ and Cyprus Arc is particularly problematic (Rojay et al., 2001; Över et al., 2004a; Oguchi et al., 2008; Duman and Emre, 2013; Mahmoud et al., 2013).

In the study area (Figure 1), the EAFZ cuts across the northern Amanos Mountains diagonally and reaches the Mediterranean (McKenzie, 1970; Dewey et al., 1973; Gülen et al., 1987; Karig and Kozlu, 1990; Kempler and Garfunkel, 1991; Westaway, 1994; Arger et al., 2000; Koçyiğit and Beyhan, 1998; Yurtmen et al., 2000; Robertson et al., 2004) (Figure 2a). According to several authors, this fault zone is connected to Cyprus Arc in the Mediterranean (Dewey and Şengör, 1979; McKenzie, 1976; Muehlberger and Gordon, 1987; Hall et al., 2005; Kempler and Garfunkel, 1994; Kahle et al., 2000) (Figure 2b). However, the EAFZ has also been shown either to tip-out close to Türkoğlu (which is located to the south of Kahramanmaraş) (Chorowicz et al., 1994; Lovelock, 1984; Görür et al., 1984; Perinçek and Çemen, 1990; Yürür and Chorowicz, 1998) (Figure 2c), or to extend into the Karasu Rift Valley (Arpat and Şaroğlu, 1973; Şengör et al., 1985).

In addition, alternative models have the EAFZ directly connecting with the northern extent of the DSFZ in Amik Plain (Allen, 1969; Arpat and Şaroğlu, 1973; Kelling et al., 1987; Kiratzi, 1993; Rotstein, 1984; Şengör et al., 1985; Rojay et al., 2001; Adıyaman and Chorowicz, 2002; Över et al., 2002; 2004b; Westaway, 2003; 2004; Seyrek et al., 2007; Herece, 2008; Duman and Emre, 2013; Emre et al., 2013; Seyrek et al., 2014) (Figure 2d).

In spite of this long-standing debate, a definitive location for the northern part of DSFZ, northeastern part of Cyprus Arc and southwestern part of EAFZ is still a standing question. This current study intends to discriminate between the tectonic faults and fault dynamics of the region by analyzing the morphometric characteristics of the deformation caused to alluvial fans -young

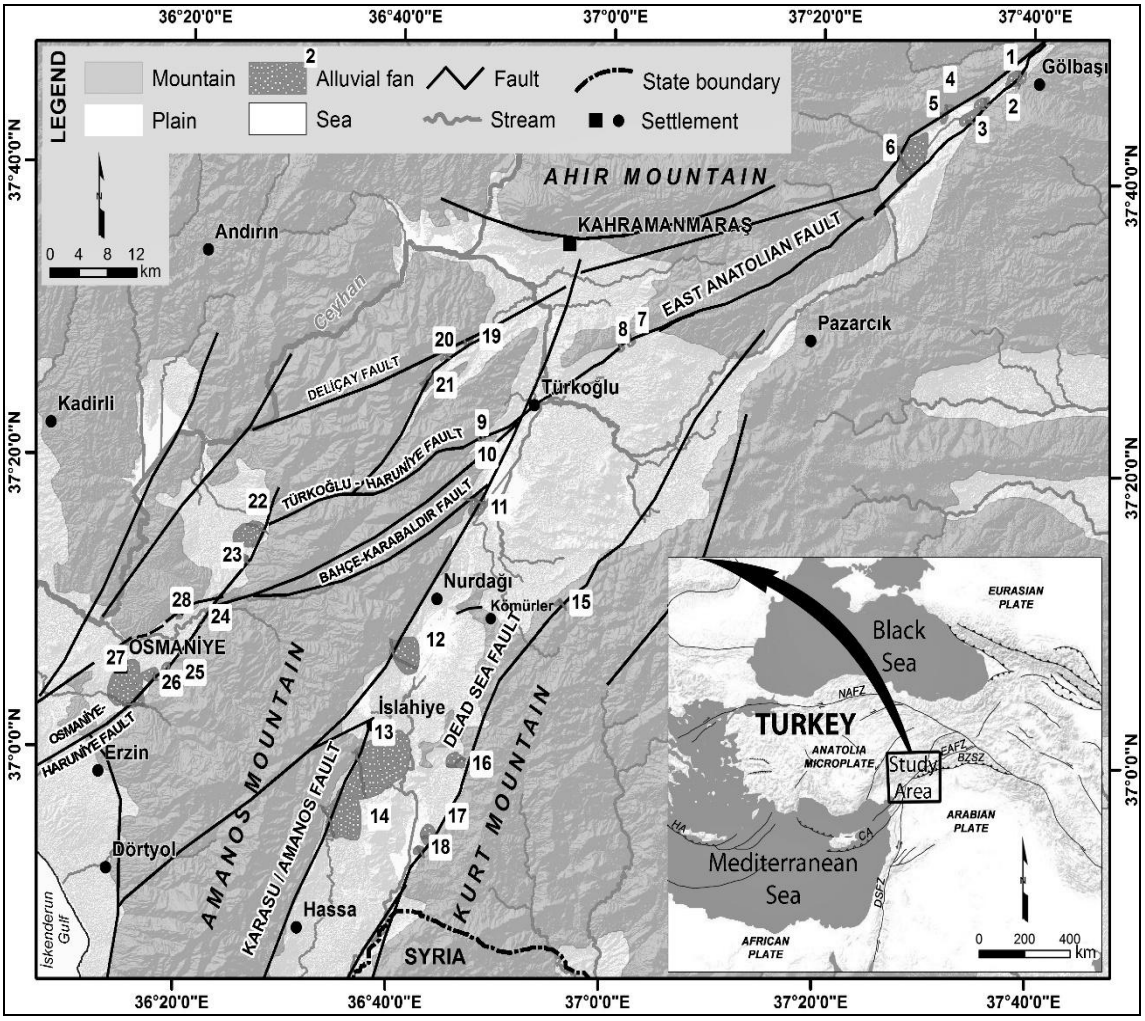

Figure 1: Location map of the study area and its close vicinity, alluvial fans and the position of main faults based on their names in the literature. (Allen, 1969; McKenzie, 1970; Arpat and Şaroğlu, 1973; Dewey et al., 1973; McKenzie, 1976; Dewey and Şengör, 1979; Şengör and Yılmaz, 1983; Görür et al., 1984; Şengör et al., 1985; Yılmaz et al., 1985; Perinçek and Çemen, 1990).

geomorphological units - by active and neo-tectonic faulting in the study area (Tatar et al., 2004). The impact of sea level change is limited to the structural characteristics of the alluvial fans, especially the Quaternary fans located away from the present-day shoreline effects, with the exception of toe trimming (Harvey et al., 2005). At the same time, tectonic movements have a determinative role on the shapes, slopes and fluvial morphological developments of alluvial fans and leave readable traces behind (Beaty, 1961; Hooke, 1967; Harvey, 1990, 2002; Pope and Wilkinson, 2005). Correct interpretation of these traces will facilitate the recognition of the underlying structural controls.

Segments of tectonic lines of different character have been clearly identified through a different method previously not used in this area (Reilinger et al., 1997; Westaway et al., 2008; Meghraoui et al., 2011; Tarı et al., 2014) allowing the discrimination of mean tectonic belts and plate boundaries based on the association of the fault systems displaying similar behavior.

METHODOLOGY

The digital elevation model of the study area was generated from and the ASTER GDEM 15 m resolution Digital Elevation Model (DEM) (METI and NASA) using ArcMap 10.1 (ESRI). Sections of 1/25,000 scaled topographic maps prepared by the General Command of Mapping (Turkey) were also used to identify geomorphological units and determine the borders of alluvial fans. Contour line spacing of 10 m was generally used with 5 m spacing where more detailed information was needed. Geological maps of the area scaled 1/100,000 (Herece, 2008) and 1/500,000 were also used to locate the alluvial fans (MTA, 2002). The

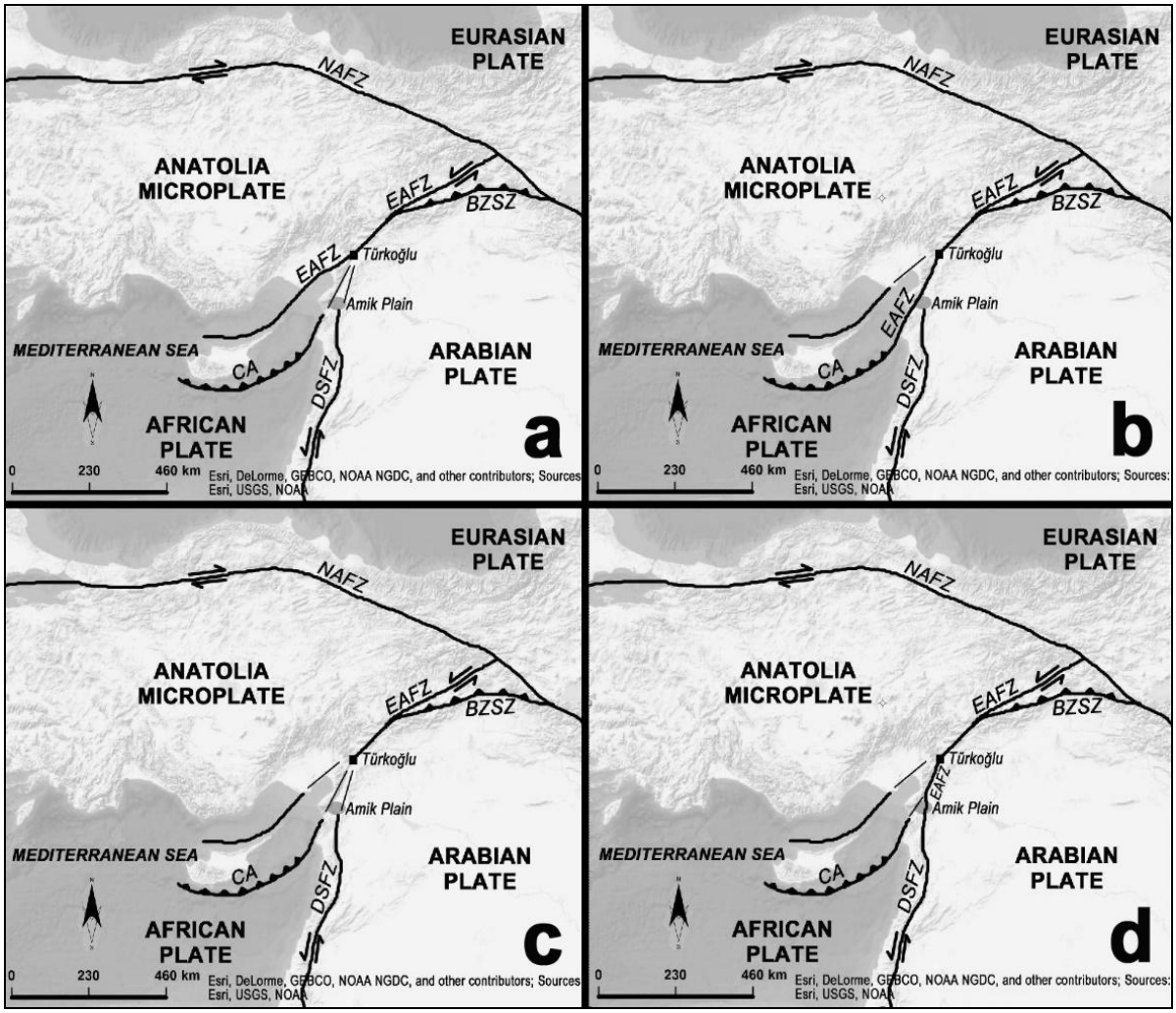

Figure 2: Some different models about the direction of ESFZ and plate boundaries in the study area. **(a)** McKenzie, 1970; Dewey et al., 1973; Gülen et al., 1987; Karig and Kozlu, 1990; Kempler and Garfunkel, 1991; Westaway, 1994; Arger et al., 2000; Koçyiğit and Beyhan, 1998; Yurtmen et al., 2000; Robertson et al., 2004. **(B)** Dewey and Şengör, 1979; McKenzie, 1976; Muehlberger and Gordon, 1987; Hall et al., 2005; Kempler and Garfunkel, 1994; Kahle et al., 2000. **(C)** Chorowicz et al., 1994; Lovelock, 1984; Görür et al., 1984; Perinçek and Çemen, 1990; Yürür and Chorowicz, 1998; Dilek, 2010. **(D)** Allen, 1969; Arpat and Şaroğlu, 1973; Kelling et al., 1987; Kiratzi, 1993; Rotstein, 1984; Şengör et al., 1985; Rojay et al., 2001; Adıyaman and Chorowicz, 2002; Över et al., 2002; 2004b; Westaway, 2003, 2004; Hardenberg and Robertson, 2007; Seyrek et al., 2007; Herece, 2008; Duman and Emre, 2013; Seyrek et al., 2014).

position of significant faults in the study area was based on the reports of Yalçın (1980), Yılmaz (1984), Lyberis et al. (1992), Yürür and Chorowicz (1998), Rojay et al. (2001), MTA (2002), Yurtmen et al. (2002), Över et al. (2004c), Albora et al. (2006), Boulton and Robertson (2008), Herece (2008), Karabacak et al. (2010, 2012), Emre et al. (2012a, b), Duman et al. (2012) and Yönlü et al. (2013).

In addition to fundamental characteristics, such as surface area, length, width and average slope measurements (easily derived from the DEM), concavity index, best-fitting ellipse and sinuosity index analyses were undertaken for each fan. The fan apex is taken as the point at which the stream emerges from the mountain front; this is where sediment deposition will commence when the main body of the fan is actively accumulating. The fan toe is located as the point at which active channel leaves the alluvial fan deposits at the downstream extent.

Concavity index was calculated using two different methods. The first method is based on the relationship between alluvial fan profiles and the line in the direction of fan apex-fan toe (Langbein, 1964; Demoulin, 1998). In this analysis, the distance of profile slope along the direction between the fan apex and fan toe and also the ratio of the distance of the profile slope to the fan floor at the same point were calculated at the mid-point of the profile (h_{mid} / H_{mid}) according to both Langbein (1964) method and at the

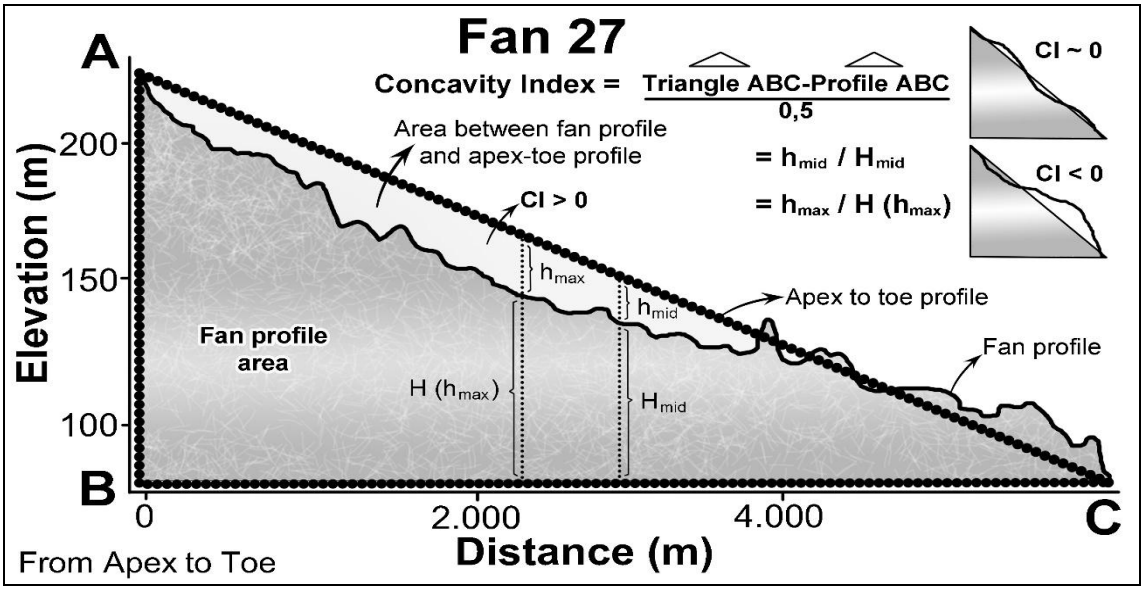

Figure 3: Representation of variables used in concavity index calculation methods used in fan 27 calculations.

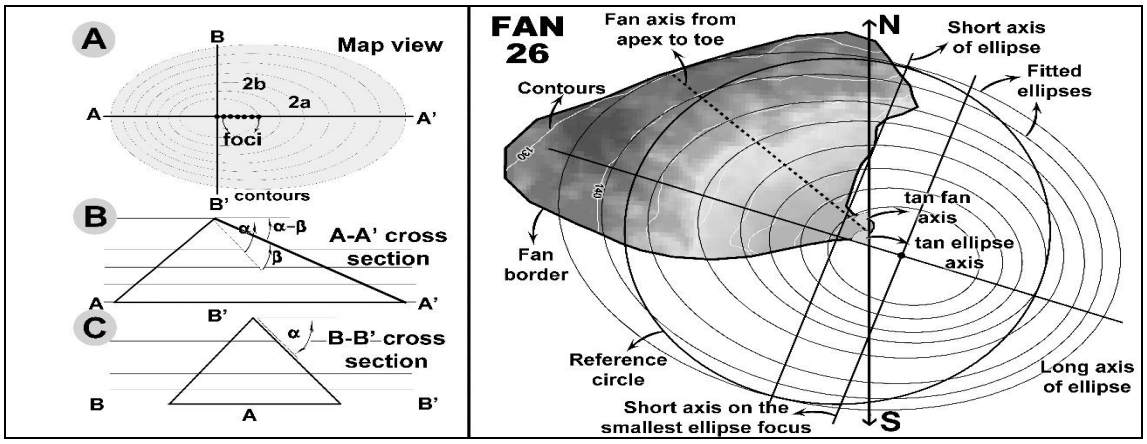

Figure 4: Model that represents alluvial fan dimensions and distortion angles according to Pinter and Keller(1995a) and its implementation on fan 26 as an example. According to Goswami et al. (2009), parameters used in the direction and distortion angle of the tectonic distortion of the alluvial fans can be observed on Fan 26 sample.

point of maximum difference between alluvial fan profile and fan apex-fan toe directional line (h_{max} / H(h_{max}) according to the method of Demoulin (1998) (Figure 3).

The second method used in determining the concavity index is based on proportioning the area bordered by the alluvial fan profile slope in the ordinate plane (fan profile area) and the area of the triangle (triangle ABC) whose hypotenuse is made of the line in the direction of fan apex-fan toe (Demoulin, 1998; Molin et al., 2004; Zaprowski et al., 2005) (Figure 3). This method was implemented through raster data analysis which identifies each profile in equal dimensions to ensure preservation of the ratio between profile areas calculated. Since the calculations based on area ratio remove problems that can be caused by the irregular topographic surface of the alluvial fan profile, they ensure more accurate results. Therefore, concavity index values obtained through area ratio method were used in interpreting morphometric analysis results. But in order to cross-check the results of the second method the dataset obtained by the first method is also considered.

Another morphometric analysis method implemented on the alluvial fans in the study area is the best-fitting ellipse method (Pinter and Keller, 1995a; Burbank and Anderson, 2001). This method can be summarized as the measurement and interpretation of dimensions related to ellipses that are nested according to the correlation of contour lines on alluvial fans, allowing a simplified geometric form of the fans to be constructed (Figure 4). Identification of morphometric parameters such as the curve axis of the concave region of the alluvial fans, apex to

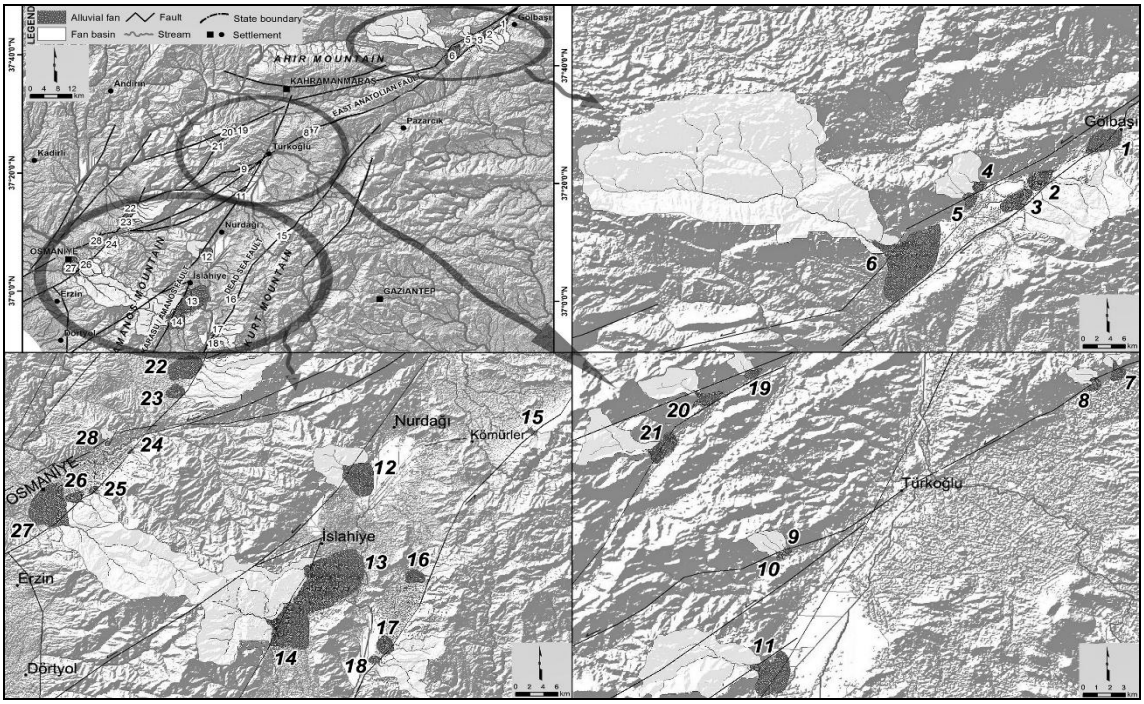

Figure 5: Alluvial fans, their basins and main faults in the study area.

toe direction of the axis and arc width is possible through the analyses of the ellipses. Like the ratio of short and long axes of the established ellipses, the ratio of the short and long axes that are stretched to the most outer ellipse by going through the center of the most inner ellipse provides the angular value of the distortion displayed as regards to equilateral fan that would be created under normal conditions (Figure 4). A reference circle, placed inside and tangent to the biggest ellipse was utilized to facilitate the measurements and increase accuracy. In addition, since the rotational distortion of the fans was in question, measurements were conducted to calculate the difference between the fan's apex-toe directional axis and long axis of the ellipses that belonged to the fan (Ron et al., 1984; Goswami et al., 2009) (Figure 4). The arc of the two axes and the tan α between them were calculated to identify angular value and direction.

While establishing long axis profiles for the fan, normalized thalweg profile for the river that formed the fan was also drawn. By representing these two profiles together, information can be obtained about the erosional and depositional activities of the river on the fan. This is achieved by identifying the sections that fall above and below the active channel with reference to the fan surface profile between the fan apex-fan toe, using the long profile of the current channel. In this context, evidence regarding the tectonic activities that caused deformation on the alluvial fan was examined based on these erosional and depositional areas.

The last parameter considered in the framework of the morphometric analyses of alluvial fans is the sinuosity index ratio (Mueller, 1968; Leopold et al., 1964). This analysis is based on the ratio between peripheral length of the right-angled triangle formed by the fan apex-fan toe directional line on the hypotenuse and circumference length of the right-angled triangle formed by the alluvial fan profile curve. With this method, it was possible to obtain information about the sinuosity ratio on the surface of each fan through apex-toe profiles.

Finally, we assume that the climatic controls on the fan development will be similar for all the studied locations due to the similarity of the focused geographic area of the study region. Palaeoclimate data suggests that during glacial periods the region was more arid than the present with 2 to 10 times less rainfall than the current 500 to 1000 mm/yr (Robinson et al., 2006). Also given that the majority of the fans are > 70 km inland, we assume that relative base-level changes are the result of local tectonics not the upstream propagation of Quaternary base-level changes in the Mediterranean Sea.

RESULTS

In total, 28 alluvial fans were selected for study on three main controversial tectonic lineaments, the East Anatolian Fault Zone, Dead Sea Fault Zone and Osmaniye section consisting of nine different fault segments (Figures 1 and 5). They also have different shapes, sizes and morphometric characteristics (Table 1). Systematically, all fans are

Table 1: Morphometric characteristics of the alluvial fan in the study area and concavity index values calculated with three different methods.

S/No	Fan area (km^2)	Fan length (m)	Fan width (m)	Distance mid. to toe (m)	Apex Elevation (m)	Toe Elevation (m)	Mid. fan Elevation (m)	Fan profile H (m)	Mid. profile h (m)	Concavity (h_{mid}/H_{mid})	Concavity (h_{max}/H_{max})	Concavity Tri. ABC-Prfl. ABC/0.5
1	3.851	1852	3250	1018	902.1	879.6	892.4	22.5	11.25	0.138	0.078	1.09
2	2.159	1623	2225	1011	890.3	871.0	876.0	19.3	9.65	-0.482	1.104	0.74
3	2.678	1562	2270	591	898.9	871.0	881.0	27.9	13.95	-0.283	0.638	0.84
4	0.711	930	1159	277	983.2	871.0	904.5	112.2	56.10	-0.403	0.479	0.66
5	1.038	1064	1440	349	959.6	871.0	899.0	88.6	44.30	-0.368	0.407	0.73
6	17.094	4944	7103	1645	908.0	871.0	881.2	37.0	18.50	-0.449	1.000	0.71
7	0.792	1385	1023	423	621.4	575.6	598.0	45.8	22.90	-0.022	0.215	0.95
8	0.520	766	979	345	625.5	557.7	587.3	67.8	33.90	-0.127	0.133	1.07
9	0.201	480	516	334	588.2	534.1	559.6	54.1	27.05	-0.057	0.046	1.04
10	0.193	491	528	222	598.2	528.8	555.2	69.4	34.70	-0.239	0.260	0.86
11	4.879	2551	3195	1188	501.3	471.0	485.8	30.3	15.15	-0.023	0.773	0.91
12	14.058	5134	3985	2799	549.0	476.1	485.5	72.9	36.45	-0.742	1.043	0.46
13	49.729	6292	10537	3741	566.0	429.2	473.4	136.8	68.40	-0.354	0.571	0.73
14	24.208	5929	6261	3376	506.8	428.4	446.0	78.4	39.20	-0.551	1.422	0.69
15	0.776	1312	1482	560	796.8	671.9	710.0	124.9	62.45	-0.390	0.638	0.86
16	3.603	2459	1772	1039	510.2	433.0	456.0	77.2	38.60	-0.404	0.911	0.74
17	4.105	2301	2406	943	434.7	398.3	408.3	36.4	18.20	-0.451	0.855	0.62
18	1.168	1417	1542	594	430.1	398.3	403.8	31.8	15.90	-0.654	1.791	0.45
19	0.476	832	1166	452	681.6	594.9	632.3	86.7	43.35	-0.137	0.233	0.87
20	1.190	1426	2204	375	895.6	682.1	754.6	213.5	106.75	-0.321	0.359	0.77
21	2.015	1918	2289	901	825.6	736.4	769.9	89.2	44.60	-0.249	0.265	0.82
22	10.616	4324	3989	1781	392.9	294.8	328.4	98.1	49.05	-0.315	0.769	0.79
23	3.372	2105	2000	645	380.2	313.1	336.5	67.1	33.55	-0.303	0.276	0.90
24	0.178	380	642	169	191.4	157.8	170.3	33.6	16.80	-0.256	0.364	0.97
25	0.910	1113	1369	330	224.9	159.7	185.9	65.2	32.60	-0.196	0.430	0.76
26	2.522	1933	1925	697	220.9	114.1	144.4	106.8	53.40	-0.433	1.137	0.65
27	22.352	5795	5982	1710	224.2	92.00	139.9	132.2	66.10	-0.275	0.327	0.85
28	0.307	629	639	201	196.7	153.9	180.3	42.8	21.40	0.234	0.053	1.19

categorized and analyzed according to their tectonic belts.

East Anatolian Fault Zone

Fans numbered 1, 2 and 3 are located on the southern fault branch of one of the two faults, regarded as elements that belong to Eastern Anatolian Fault trending northeast to southwest starting north of Gölbaşı (Figure 1) (Dewey and Pindell, 1985; Barka and Reilinger, 1997; Çıplak and Akyüz, 2005; Westaway et al., 2008; Erkmen et al., 2009; Karabacak et al., 2012; Yönlü et al., 2013). However, many previous studies (Ketin, 1965; Lyberis et al., 1992; Westaway, 2003; Yılmaz et al., 2006; Karabacak et al., 2012; Khalifa et al., 2018) state that this lineament maybe a thrust zone representing the continuation of the Bitlis-Zagros Suture Zone.

Therefore, there is uncertainty regarding the nature of the fault crossing these three fans. By contrast, the northern segment of the East Anatolian Fault (fans number 4, 5 and 6) (Figure 1) is not under the influence of the Bitlis-Zagros Suture Zone. Therefore, it is possible to separate deformation effect of these two branches if the geodynamic

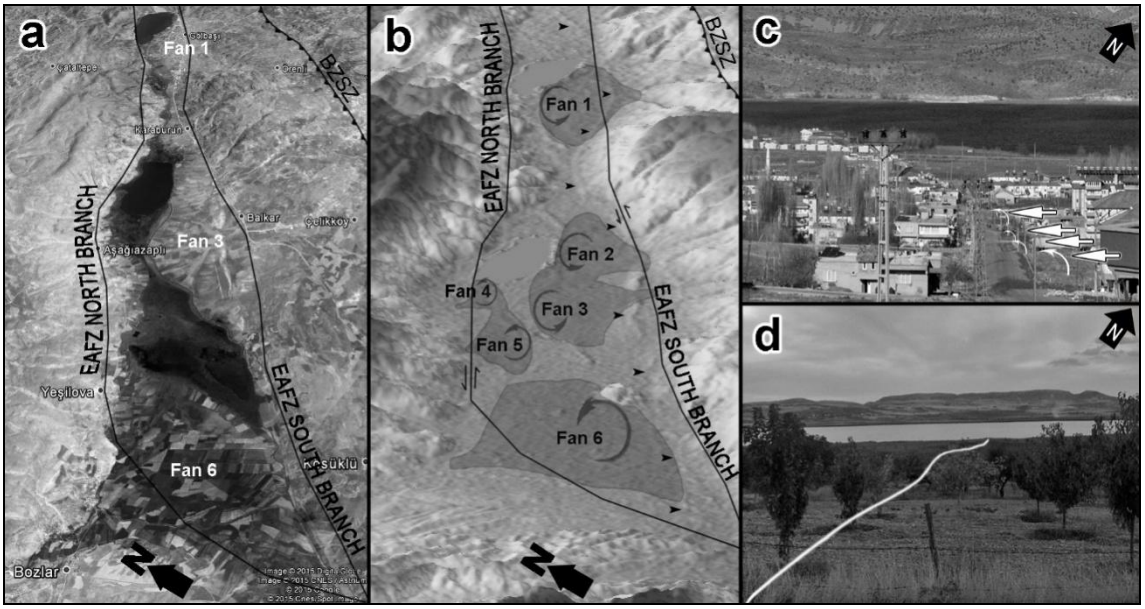

Figure 6: a) Google Earth image of the fans 1 to 6 located area; b) Continuing sinuosity lines along main faults (small black arrows) and their position according to fans and ellipse axis rotation direction fit to main faults on DEM; c) Folds right to apex-toe profile on fan 1; d) Undulated alluvial deposits in fan 3 (from middle of fan to toe).

controls are different by comparing surface profiles of these two groups of alluvial fans (Figure 6a).

All the fans have high short to long axis ratios of > 0.75 and high fan profile sinuosities (Table 2). However, there are a range of rotations recorded from a minimum of 8° for fan 6 to a maximum of 44° for fan 3 (Figure 6b). The main variations between these six fans can be observed on the long profiles. Fans 4 and 5 have concave up smooth profiles whereas the other fans show pronounced apex to toe profile irregularities and profile convexities within the thalweg. These convexities are up to 10 m high on fans 1 to 3 but < 5 m in height on fan 6 (Figure 6c and d).

By contrast, fans numbered 7 and 8 are located on the southernmost EAFZ segment, which is believed to continue southwest from the northeast by-passing Gölbaşı Basin and extendings as far as Türkoğlu. Fans 7 and 8 share similarities with fans 1, 2 and 3, in terms of overall profile surface characteristics and profile surface-thalweg relationships (Figure 7); especially in fan 8, which overall has a convex shape. The short/long axis ratios for best fit ellipses drawn for fans 7 and 8 are 0.573 and 0.648, respectively. The fan surfaces show a 16° and 11° sinistral rotational movement, and have sinuosity ratios of 0.943 and 0.956 (Table 2).

Interpretation

Examination of surface and current stream bed profiles of the fans -by taking all the conditions earlier mentioned shows an obvious inconsistency between fans number 1, 2 and 3 and fans 4, 5 and 6 (Figure 7). Fans 1 to 3 show profile convexities in the channel profile suggesting that all three fans are located on the same fault segment with convex sinuosity bands indicating that the fault has a component of reverse motion (Figure 6c and d). It is because during the last fifty years local base level (Gölbaşı and Azaplı, lakes) for fans 1 to 6 is almost the same (EİE, 2005; rasatlar.dsi.gov.tr). However, some new progressive fan penetration in the lakes (Figure 9) is on. This could be the result of fan surface uplift.

In contrast to the southerly fan surfaces with rough sinuosity, the fans on the north branch present simpler profiles. When the river beds embedded in the folds (through similar process in antecedent gorge forming) observed in fans number 1, 2 and 3 were taken into consideration it is possible to claim that the lengthwise profiles of the fans carry traces of compressional regime. At this point, only fan number 6 presents different kinds of surface profile lines suitable to its own multichannel fed position.

On the other hand, contrary to clear and wide convex folds observed in southbound fan profiles, there is a simple concavity in the fans observed in the north branch (Table 1). In this case, it is understood that the profile slope which is supposed to gradually decrease from apex to toe (Blissenbach, 1954; Bull, 1964) is highly deformed in the fans located in the south branch. Although only the profile that belongs to fan number 1 is convex while others are concave; three distinct concave folds can be distinguished on the surface profiles of all the fans in the south branch (fans number 1, 2, and 3). Similarity in the shape of the deformation suggests that all three fans are located on a different tectonic deformation zone than fans 4, 5, and 6

Table 2: Values for the distortion directions and distortion ratios obtained from best fitted ellipse analyses of alluvial fans in the study area and sinuosity index values of fans.

S/No	Short axis (m)	Long axis (m)	Short axis/Long axis	Smallest ellipse focus axis (m)	Smallest ellipse focus axis/Long axis	Fan axis direction (According to 90° North)	Ellipse axis direction (Accordingto 90° North)	Ellipse axis rotation degree and direction	Fan profile sinousity ındex
1	3257	3789	0.860	3243	0.856	33° W	71° W	38° L	0.847
2	2448	3060	0.800	2465	0.806	63° W	75° W	12° L	0.868
3	2793	3598	0.776	2742	0.762	42° W	86° W	44° L	0.918
4	1725	2281	0.756	1719	0.754	139° E	123° E	16° L	0.969
5	1924	2502	0.769	1907	0.762	127° E	107° E	20° L	0.973
6	6742	8400	0.803	6485	0.772	112° E	104° E	8° L	0.788
7	1335	2329	0.573	1326	0.569	166° E	150° E	16° L	0.943
8	1474	2273	0.648	1455	0.640	176° E	165° E	11° L	0.956
9	805	1486	0.542	801	0.539	166° E	151° E	15° L	0.981
10	1069	1506	0.710	1062	0.705	139° E	135° E	4° L	0.975
11	3459	4458	0.776	3312	0.743	131° E	117° E	14° L	0.852
12	5246	8853	0.593	5159	0.583	124° E	82° E	42° L	0.932
13	11714	14791	0.792	11524	0.779	136° E	118° E	18° L	0.929
14	6589	9433	0.699	6154	0.652	123° E	110° E	13° L	0.850
15	1690	2596	0.651	1641	0.632	51° W	55° W	4° L	0.962
16	3326	4934	0.674	3264	0.662	95° W	96° W	1° L	0.955
17	3138	5159	0.608	3087	0.598	48° W	46° W	2° R	0.926
18	2309	3365	0.686	2303	0.684	40° W	42° W	2° L	0.924
19	1930	2239	0.862	1928	0.861	133° E	117° E	16° L	0.978
20	1842	2549	0.723	1796	0.705	139° E	133° E	6° L	0.970
21	2958	3798	0.779	2872	0.756	95° E	60° E	35° L	0.969
22	4370	5638	0.775	4173	0.740	68° W	56° W	12° R	0.900
23	3535	3993	0.885	3440	0.862	67° W	65° W	2° R	0.884
24	1051	1590	0.661	1042	0.655	48° W	36° W	12° R	0.969
25	2177	2496	0.872	2165	0.867	38° W	47° W	9° L	0.954
26	2453	3259	0.753	2377	0.729	44° W	71° W	27° L	0.949
27	7587	9491	0.799	7309	0.770	40° W	47° W	7° L	0.888
28	1038	1732	0.599	1032	0.596	174° E	168° E	6° L	0.970

(Figure 7).

The best fitted ellipses formed for the first six fans that are studied present a short/long axis ratio in 0.756 and 0.860 interval. These values point to fans with comparatively high roundness ratio at a regional scale (Table 2). Therefore, it is not possible to define the tectonic regime based on the amount of distortion, which will increase in favor of long axis based on the impact of the normal faults (Pinter and Keller, 1995b). On the other hand, sinistral (counter clockwise) rotational movement changing between 8° and 44° was detected in the fans

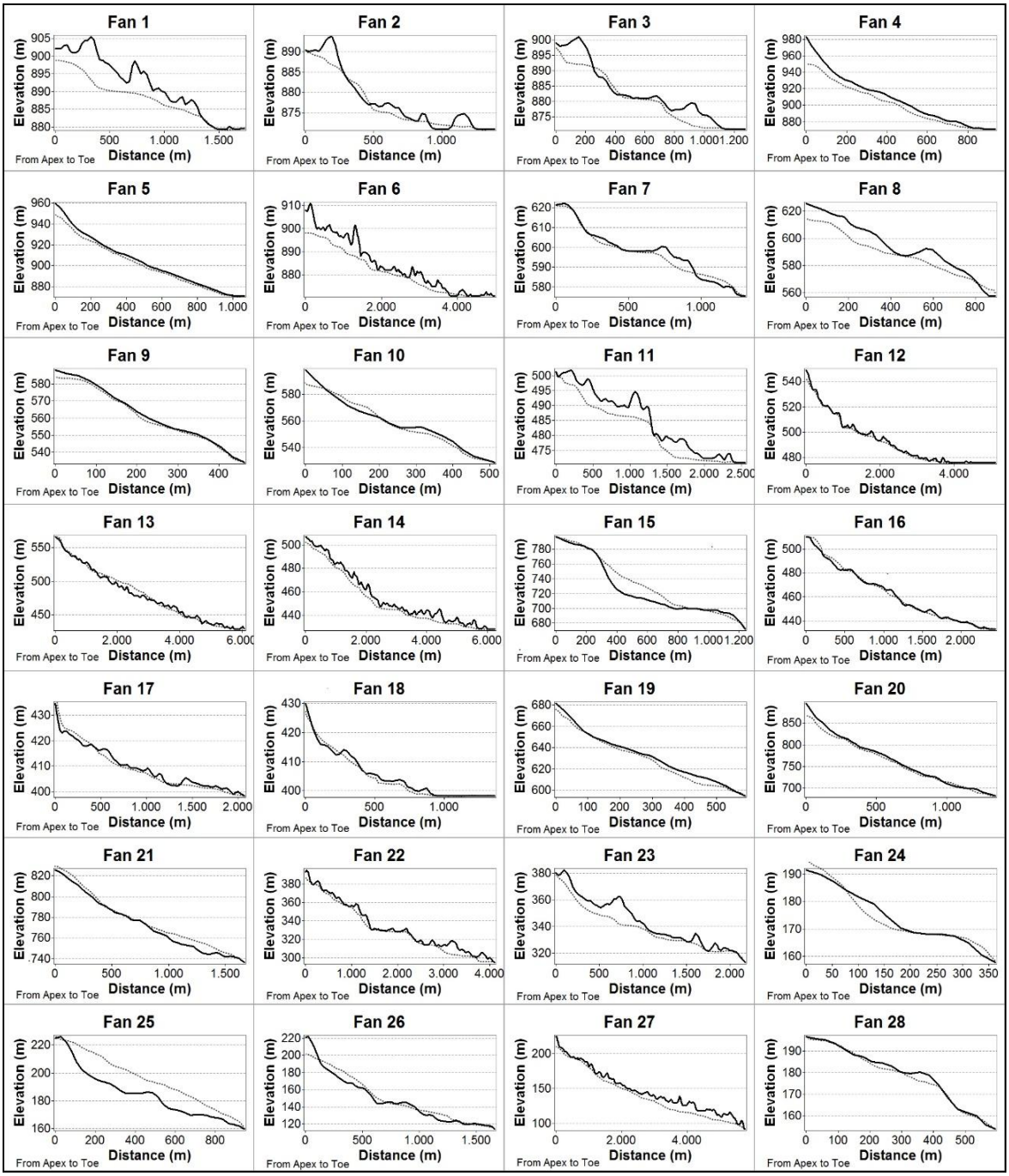

Figure 7: Apex-toe (smooth line) and thalweg (dashed line) profiles of the alluvial fans in the study area.

numbered from 1 to 6. This movement signifies the fact that fan shifted to the right compared to the long axis of the ellipses that best fitted the directions of the contour lines that belonged to convex profile. Although partial impact of slope direction of the plain floor where the fan was formed was not ignored, it is apparent that the main factor is the direction of the lateral components in the fault slip. Therefore, propelling the fan body to the left with left lateral slip causes the formation of a deposit field at a lower altitude and results in the development of a fan convex profile.

These actions generate new segments to the right in a continuous manner and shaping of the convex fan body on the right while the left axis that corresponds to the pointed ends of the ellipse stay on the left. Therefore, faults with vertical slip that are the left lateral slip or left lateral components of the fan body intersect with faults with vertical slip in all fans from 1 to 6 (more in fans number 1

and 3). Earthquake focal mechanism analyses conducted on the faults in the region and earthquake slip data analyses obtained from fault planes for previous earthquakes and geodetic data obtained from around the vicinity of fault planes support this interpretation (Yürür and Chorowicz, 1998; Yılmaz et al., 2006; Yönlü et al., 2013).

The high short-long axis ratios observed on fans 7 and 8 may be due to comparatively high slopes of the plain floor where the fans are located. However, the presence of convex folds can be regarded as an indicator of compressional regime and deeply embedded thalweg lines which are more distinctive where the folds are located (Figure 7). In short, it is observed that while the fans were subjected to continuous and effective deformation considering their respective 3.31 and 8.85% apex-toe slopes, they also continued their development in favor of long axis with the help of new sediments added to fan apex vicinity due to high hydrologic energy. Tendency to escape southwest triggered by the north northwest-south southeast directional compression determined through kinematic analysis and geodetic investigations decreased the impact of the sinistral lateral slip of the faults that intersect the fans (Över et al., 2004c; Reilinger et al., 2006; Karabacak et al., 2012; Mahmoud et al., 2013). As a result, sinistral rotational movement of the fans weakened and the fans with little change in the foot position showed a tendency to extend backwards.

Dead Sea Fault Zone

Fans 11, 12, 13 and 14, from northeast to southwest in the area between Türkoğlu and Hassa, are located along the fault that borders the eastern margin of the Amanos Mountains (Figure 2). However, fan 11 has a different morphology compared to the other three fans. Fan 11 exhibits two clear convexities within the thalweg profile, high amplitude irregularities in the fan surface and a very high overall concavity of 0.91. Fans 12 to 14 by contrast have lower concavities and concave up channel profiles with lower amplitude and high frequency irregularities on the fan surface. All these fans have high sinuosities (> 0.85) and axis ratios in the range 0.6 to 0.8. There is also a fairly consistent fan orientation (~ 130°) (Table 2) and rotation (~ 16 °). It is interesting to note that fan 12 has slightly different values where the ellipse axis is orientated to 82° and indicates 42° of rotation. Examination of ellipses that are compatible with the fans shows that fan 12 is different from the other fans based on its low roundness. Furthermore, the thalweg profiles have convolutions compatible with fan surface profile in fans 12, 13 and 14 but apart from fan 11 where the channel is deeply incised (Figures 6 and 8a).

Fan 15, located on the fault that borders the northern Karasu Rift in the east and to the immediate east of Nurdağı (Figure 2), is represented in Figure 7 with a wide convexity on its surface, although the longitudinal channel profile is more linear in appearance. While the comparative lengthwise images of the ellipses compatible with the contour lines that formed the fan are present with 0.651 short/long axis ratios, sinuosity index value of 0.962 corresponds to a simple surface with a sinistral rotational motion of 4°.

Fans 16, 17 and 18, located to the south of fan 15, are situated on the fault that separates Kurt Mountain and Antakya-KahramanmaraşGraben (Karasu Rift) and have broadly concave channel profiles and fan surface with minor irregularities. Fan 18 has a concavity of 0.45, whereas fans 16 and 17 have higher concavities or 0.74 and 0.62, respectively. Best fit ellipse analyses of the fans present comparatively lower distortion ratios such as 0.662, 0.598 and 0.684, of 16, 17 and 18, respectively (Table 2) and only minor evidence of long axis rotation.

Interpretation

Fan 11 has been deformed due to shear effect of the fault (Bahçe-Karabaldır Fault (Yalçın, 1980; Günay, 1984) that strikes southwest and diagonally crosses the Amanos Mountains. Fans 12, 13 and 14 with stable and simple concave profiles points to a distinct extensional regime. Fan profiles are slightly concave but the faults that cross fan 11 result in distinctive convexities indicating complete push-up. Hence, clockwise motion of the block between Bahçe-Karabaldır and Dörtyol-İslahiye faults (Günay, 1984) that diagonally cut Amanos Mountains in the northeast-southwest direction strengthened sinistral lateral slip in the fault that cuts through fan 12 (Günay, 1984). The lengthwise form of this fan should be assessed together with the amount of rotational movement which is also significantly different as compared to other fans because these two parameters may provide the evidence for the existence of a different block tectonics in the region where fan 12 is located.

Results of kinematic analyses between traces of previous earthquakes and fault planes also support these views (Över et al., 2004b, c). Geodetic data of the region provides similar descriptions about slip directions as well (Reilinger et al., 2006; Mahmoud et al., 2013). Therefore, as the basis of block motion, it would not be wrong to assert the existence of south-north or even south southeast-north northeast directional compressional impact on the northeast-southwest steering faults that border the block.

The concave profile of fan 15 may be an indication of extensional regime because of a fault scarp which transects the fan (Figure 8b). However, the extension here is not only associated with the normal components of the fault it is located on but with the left lateral motion related to a possible fault that reaches the north of the fan by diagonally cutting the rift valley from the south of Nurdağı. Faulting in the vicinity of Kömürler settlement between Nurdağı and

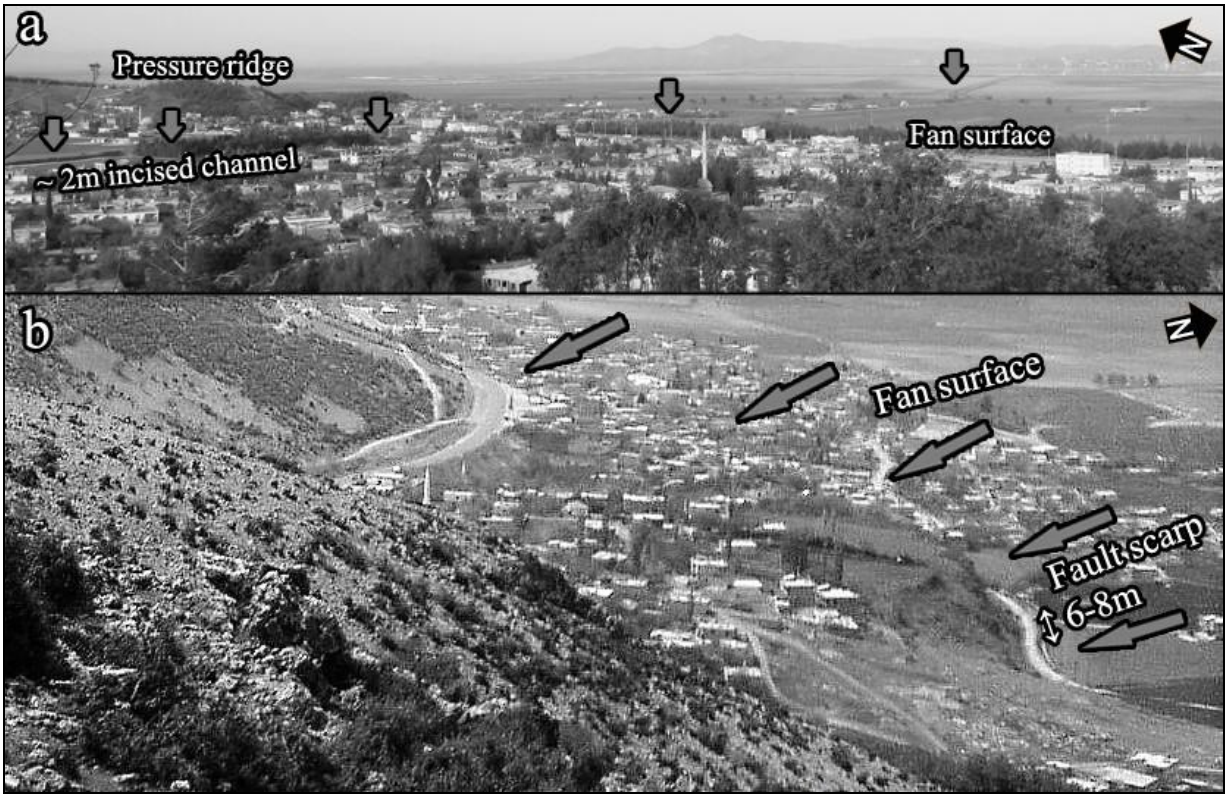

Figure 8: (a) Approximately, 2 m incised main channel on fan 11; b) Meanly 6 to 8 m vertically slipped fault scarp near fan 15.

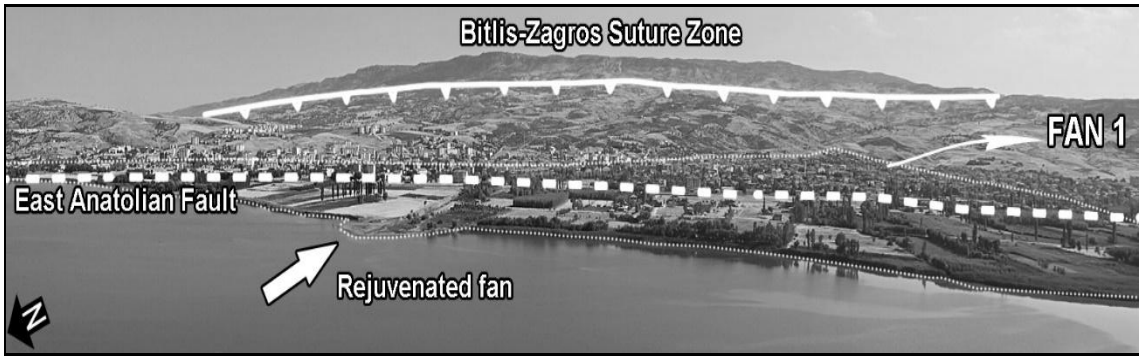

Figure 9: Location of Bitlis-Zagros Suture Zone and East Anatolian Fault in the southern Gölbaşı Basin where fan 1 is located. Regeneration is observed in the fan due to compressional regime even though local floor level does not change.

fan 14, Lyberis et al. (1992), Yurtmen et al. (2002) and Över et al. (2004b) provides support for the existence of such a fault. Also the fact that independent of fan surface, the thalweg line does not reflect the same concave undulation with the fan profile is an indication that apex-toe line of the thalweg and fan are positioned in the different sides of the fan. The low angle of rotation identified in the fan shows that lateral slip is sinistral but with less fierceness (Table 2). As a result, this fan acts as a confirmation that the eastern rift valley fault is shaped by the extensional regime and the fault exhibits left lateral slip and a vertical component of motion (Yurtmen et al., 2002; Karabacak et al., 2010).

Fan 18's 0.45 ratio concavity is suggestive of an extensional regime contrary to the indistinct ridges possibly caused by pressures that change direction and presents the general characteristic of tectonic activity in this part (Table 1). On the other hand, no significant discordance was detected between thalweg and fan surface profile other than the small-scale irregularities earlier mentioned. Discordance in the areas that correspond with small folds shows that these folds are recently shaped

because surface flow has not removed these small topographic elements on the fan surface but the river bed was embedded here as an antecedent. Low distortion ratios such as 0.662, 0.598 and 0.684, respectively (Table 2) also suggest that the extension affecting the fans is not significant. Directions of fans' apex-toes axes and best fitted ellipse axes are also very close whereas lateral slip impact is almost non-existent.

Therefore, evidence shows that lateral motion of the tectonic line that fans 16, 17 and 18 are situated upon decreases and it mostly corresponds to an area where vertical motion shaped by normal faults increases. This view also supported by literature (Lyberis et al., 1992) is parallel to data related to directions of slip as well (Reilinger et al., 2006; Mahmoud et al., 2013).

Osmaniye to Türkoğlu Fault Zone

Fans 9 and 10 are located on one of the fault zones (Türkoğlu-Haruniye fault (Günay, 1984) that intersect Amanos Mountains in the northeast-southwest direction to the southwest of Türkoğlu. Fan 9 is slightly convex; while fan 10 is slightly concave (Figure 7). Both fans have a concave undulation in their middle segments and there are no significant discrepancies between fan and thalweg profiles. Examination of long/short axis ratios of the ellipses drawn for the fans shows the ratio of 0.542 for fan 9 which is located where fault is closer to Türkoğlu whereas the ratio for fan 10 which is located further southwest is higher with 0.710 (Table 2). Additionally, it is observed that 15° left rotational movement in fan 9 decreases to 4° in fan 10.

Surface profile of fans 19, 20 and 21 located on Deliçay Fault that cuts Amanos Mountains (Figure 2) in the northeast-southwest direction starting from the south of Kahramanmaraş (Yılmaz, 1984) are rather simple and present a monotonous concavity (Figure 7). The fact that the concavity ratio values are rather low with 0.87, 0.77 and 0.82, respectively, and with short/long axes values of the ellipses of 0.861, 0.705 and 0.756. On the other hand, 16, 6 and 35° sinistral rotational motion is detected in the fans (Table 2).

The first three of the fans 22, 23, 24, 25, 26 and 27 located on Osmaniye-Haruniye Fault that forms a part of the west border of Amanos Mountains (Günay, 1984) are positioned to the northeast edge of the fault. Fans 22, 23 and 24 have slightly concave surface profiles and also contain distinct convex folds (Figure 7). Concavity in fan 24 (0.97) is so low as to adopt almost a convex structure due to convex folds (Table 1). Thalweg profiles compatible with the surface profiles on concave areas are deeply embedded in convex areas. Fans present dissimilar results in terms of respective short/long axes ratios (0.740, 0.862 and 0.655) for ellipses that are best fitted for their contour lines (Table 2).

Surface profiles of fans 25, 26 and 27 located further southwest on the Osmaniye-Haruniye Fault are similar to those of fans 22, 23 and 24. However, concavity in these fans is more apparent and convex folds are less pronounced. Although fan surface profiles and thalweg profiles present a somewhat compatible image in fans 26 and 27, a significant anomaly is apparent in fan 25 (Figure 7). However, this feature is the result of sand quarries located in the mid-part which corresponds to the apex-toe profile line of the fan. Extensive sand intake from the region has caused a large scale depression in this region. Concavity ratios of the fans are 0.76, 0.65 and 0.85, respectively and they present a clear concave profile (Table 1). The best fitted ellipse analyses provided 0.867, 0.729 and 0.770 short/long axes ratios, respectively.

The last fan investigated in the framework of the study was fan 28 located on a fault parallel to Osmaniye-Haruniye Fault, to the immediate north of fans 25, 26 and 27. Surface profile of this fan represents a clear concavity of 1.19 as opposed to the three fans in the south (Table 1). Also, distinctive convex folds deeply embedded on the surface profile of thalweg indicate the degree of compression observed in fan 28 (Figure 7).

Interpretation

The profile form for fans 9 and 10 can be considered as an indication of normal faults because of the presence of clear concave undulations in the middle of an otherwise smooth surface profile. However, convex undulations on the fan foots in contrast of the middle fan profile concavity, which indicates compression is also present (Figure 7).

This can be interpreted that the impact of the normal component in the fault increases southwest. Therefore, it is observed that lateral movement decreases from the northeast to southwest on the fault where fans 9 and 10 are located and parallel to the literature (Günay, 1984; Yılmaz, 1984) evidence strongly point to the fact that vertical movement increases with reverse components in the foot and with normal components towards the top. In this context, the zone where fans 9 and 10 are located presents suitable images for conversion and transformation area.

Low concavity ratios for fans 19 to 21 suggest a minor component of extensional faulting (Table 1). Discordance between thalweg profiles and fan surface profiles is not apparent. Respective 0.861, 0.705 and 0.756 short/long axes values of the ellipses best fitted for fans also suggest that impact of the extensional regime decreases from northeast to southwest. Existence of a pressure ridge that limits the extension field of fan 20 is the reason for lower values in the fan. On the other hand, 16°, 6° and 35° sinistral rotational motion is detected in the fans respectively (Table 2). Therefore, when fan 20 with distorted physiology is not taken into consideration it is possible to claim that sinistral lateral slip increases its

impact southwest in this part of the study area. This result increases the possibility that the block on the north of the fault that cuts the fans verges to the west by folding towards the southwest just like in the case of the Anatolian plate. However, the fact that Deliçay Fault's lateral slip quantity of decreases towards the southwest (Yılmaz, 1984) creates question marks as to whether this block can be considered as a complete part of Anatolian plate.

Fans 22, 23 and 24 have morphologies consistent with variable tectonic control on formation. This result can be associated with differences in the dimensions of the tectonic impact that the fans are subjected to. Although, dextral rotational motion (albeit a little) is noteworthy in all fans (Table 2). The fact that west and southwest displacement of the blocks between Bahçe-Karabaldır Fault and Deliçay Fault, which diagonally cut the Amanos Mountains, created a dextral line composed of compressional impact with Osmaniye-Haruniye Fault may prepare the basis for such a right shift. The documented existence of faults with dextral lateral slip in addition to normal and reverse faults in the fan area supports this view (Över et al., 2004d).

The morphology of fans 25 to 27 can be interpreted in terms of decreasing compression and fierceness of deformation. However, sinistral rotational motion of 9, 27 and 7° was calculated for the fans respectively and it was concluded that left lateral slip with decreased fierceness existed for the faults that cut the fans (Table 2). Gürsoy et al. (2003) also supports this kind of movement, but 27° left shift calculated for fan 26 is based on the existence of a tectonic deformation zone other than the faults in the fan formation mechanism. Existence of a north-south bounding fault that diagonally cuts this fan was found and it was observed that both lateral and vertical motions in this fault affected the left side more compared to fan's apex-toe direction. Existence of such active faults in the region is compatible with the mechanism that was effective in the formation of Iskenderun Basin (Aksu et al., 2005; Albora et al., 2006). It is apparent that extensions of the fault that formed Iskenderun basin reached as far as the fan regions and therefore both of these regions were shaped through the same mechanism.

Fan 28 has a short/long axis ratio of 0.596 that is an indication of the fierceness of deformation in the fan. However, 6° sinistral rotational motion indicates low left lateral slip impact (Table 2). Therefore, it is possible to claim that the block on the north of the fault that cuts the fan is in motion towards the south and southwest. Since the direction of this motion is similar in the Anatolian plate, possibility of interaction may be said to increase between these motion blocks and Anatolian plate.

DISCUSSION

Morphometric analysis of 28 mountain front alluvial fans on faults and fault zones that make up the continental plate boundary between African, Arabian and Anatolian plates has provided the opportunity to compare the potential impact of active faulting upon those fans and evaluate the structure of the study area. Morphometric analysis of alluvial fans were assessed in conjunction with various geological data such as kinematic and earthquake slip data analyses obtained from fault planes of previous earthquakes and geodetic findings obtained from GPS data (Reilinger et al., 2006; Mahmoud et al., 2013), in order to shed new light on the structure and processes in this key area.

According to the analyses, many of the faults in the study area have dominantly left-lateral slip with a smaller dip-slip component of motion, mostly with a normal sense of displacement (Günay, 1984; Yılmaz, 1984) (Tables 1 and 2). Both the comparative motion of Arabian plate with respect to the African plate, and west to southwest direction of the Anatolian plate was compared to the Arabian plate support left lateral slip (Şengör and Yılmaz, 1981). However, the boundary of the Arabian plate with African plate is not purely strike-slip but transtensional in character and the junction between Anatolian and the northwest corner of the Arabian plate during its west and southwest migration has also caused the formation of normal faults (Erinç, 1973; Erol, 1983; Yılmaz, 1984). Reverse faults, whose existence can be clearly observed both on surface profiles of fans (that is, fans 9-10-11) and in kinematic analyses results such as slip traces in fault planes and earthquake focus analyses (Günay, 1984; Yılmaz, 1984; Karabacak et al., 2012), are the result of the convergence of west -southwest Anatolia to the south andthe Eurasian plate in the north in addition to the collision of Arabian and Anatolian plates. This also includes the resulting extrusion of the Anatolian plate towards the southwest along the NAFZ and the EAFZ. By contrast, the Arabian plate's rapid motion (15 mm/year) (Reilinger et al., 2006) during Oligocene-Miocene period (Gvirtzman and Steinberg, 2011) towards the north resulted in the closure of the southern branch of Neo-Tethys in the east. However, due to slower motion of African plate (5 mm/year) (Reilinger et al., 2006) the closure is not complete in the west yet. The tectonic depression in the north of Cyprus called Adana-Kilikya Basin (Şengör and Yılmaz, 1981; Koç et al., 2012) can be considered the present day foreland basin to Anatolia.

The Bitlis-Zagros suture zone in the northeast of the study area is positioned immediatly south and parallel to the EAFZ. Slope and topography on EAFZ increases as a result of this zone and convex folds are established (Figure 9). However, the EAFZ apparently limits the southerly thrust impact and prevents compression from reaching the fans that are located on the faults that provide extensions of the Gölbaşı Basin. Therefore, the existence of a contemporary thrust in southern Anatolian that is dependent on the northern motion of Arabian plate is unexpected. The thrust deemed as the continuance of

Bitlis-Zagros suture zone in the region (Alsdorf et al., 1995; Yürür and Chorowicz, 1998; Kearey et al., 2009; Romieh et al., 2009) are either fossils that were carried to the west or southwest based on the ratio of East Anatolian Fault slip or they are independent thrusts.

Although the Arabian plate continues to move northwards, the direction and style of this motion changed since the Middle Miocene (Gvirtzman and Steinberg, 2011). The plate has approximately 5 to 15 mm/year anti-clockwise rotational movement towards the north (Reilinger et al., 2006; Gvirtzman and Steinberg, 2011; Koçbulut et al., 2013). Left lateral slip is observed due to Anatolia's rapid movements towards the west and southwest although extensional thrusting is seen in the western part due to partial freedom of the south edge of the plate, while compression is observed in the north and east and dextral slip observed in the northeastern corner located between these two opposite tectonic regimes. The intersection between these domains falls along a line that reaches Hassa from Gölbaşı-Pazarcık. Particularly, the sinistral rotational movement which is partly absorbed and increased convex folds on fan surfaces of fan 7 and 8 support this situation (Figure 7). Parallel stretches of the fold axes to thrust zone located on the plate's suture zone towards the east and northeast point to the continuity of the compression (Lyberis et al., 1992). Traces of specific deformation are visible on both sides of the plate boundary where lateral motion is observed. Direction of the folds on the Arabian plate are parallel to the plate border with lateral slip and the plate is exposed to faulting shape as dipping arcs from northeast to south (Figure 10). As expected, these faults are left lateral with reverse fault components (Lyberis et al., 1992; Yürür and Chorowicz, 1998). In other words, in-plate compressional impact was compensated with faults that allow lateral deformation.

A structure divided into small blocks by concentric arcs due to Arabia's cyclical thrust is seen on the other side of the plate border. Faults that border these blocks are also sinistral like the faults located on the plate. However, reverse fault components on these faults increase proportionally to the distance from the plate (Günay, 1984; Yılmaz, 1984). Vertical component of the left lateral slip in parts closer to plate border is composed of normal faults because extension field is generated with the westward motions of the Anatolian plate which borders these blocks from the north and the west. However, further west, western parts of the blocks experience compression due to southern bound motions of Anatolia. Therefore, the small blocks in this area both move west like Anatolia with the thrust of Arabian plate and undergo compression due to southwest motion of Anatolian plate. Hence, semi-independent blocks in question are both a part of Anatolia and also compressed between plates (Figure 10) creating a complex plate boudary zone rather than a single boundary fault.

The African plate is separated from Arabian plate on the left through Dead Sea Fault Zone. Lateral slip observed in this zone as a result of African and Arabian plates' relative movements expands into inner parts of the plates on both sides of the fault zone with tectonic lines that are similar to antithetic and synthetic faults (Figure 10).

This situation is regarded as the compensation of the lateral slip in the north of Syria by distribution in the continent (Yılmaz, 1984). The Dead Sea Fault Zone can be easily followed to the east of Antakya. However, the faults in this area that reach inwards to Arabian plate make it harder to define the main fault. In this case, extending the fault towards the border of the small blocks between Arabian and Anatolian plates would be the best approach because the origin of these blocks and their eastern border is the Arabian plate. Furthermore, fans 15, 16, 17 and 18, which are located at the eastern margin of the blocks show little rotational movement, while fans 12, 13 and 14, which are located at the western margin of the blocks indicating exact divergence regime by steady concave surfaces that also include sharp concave folds verified such a scenario. Therefore, it is necessary to extend the Dead Sea Fault to Kırıkhan in a manner that will allow it to reach the Hatay/Samandağhalf-graben, which diagonally cuts eastern margin of Amanos Mountains and consists of a complex zone of active oblique-normal and strike-slip (Samadağ Fault) faulting (Boulton et al., 2006; Boulton and Robertson, 2008; Boulton and Whittaker, 2009; Karabacak et al., 2010; Gönençgil and Karataş, 2012; Seyrek et al., 2014).

The structural and topographic suggest that this fault zone is highly significant and could represent the northeastern edge of the African plate. Therefore, Cyprus Arc represents the line where African plate dips under Anatolia and the Amik Plain represents the intersection area of this line with Dead Sea Fault Zone.

The area between Cyprus Arc-Hatay Fault zone in the south and Deliçay Fault in the north is composed of a multitude of blocks that are bordered by primary faults roughly striking northeast-southwest and cross-cutting north-south oriented faults caused by the Arabian plate's sinistral rotational motion and Anatolian plate's broadly westard migration. The eastern extent of these blocks is the area where lateral motion is observed in the northwestern corner of the Arabian plate whereas the western border is composed of the fault that limits Amanos Mountains from south and as a parallel, the faults that cut İskenderun Gulf and border Amanos Mountains from the west, followed by the Anatolian plate that adopts mass characteristics starting with Karataş-Osmaniye Fault. These faults are also lines where compressional effects generated by Anatolian plate in the faults diagonally cut Amanos Mountains end. Therefore, farther than the tectonic lines such as Karasu/Amanos Fault (Karataş and Korkmaz, 2012) which looks like a transition zone between Osmaniye-Haruniye Fault and Eastern Anatolian Fault and Dead Sea Fault, the compression in the western bound blocks first decreases and then increases again towards the west and southwest.

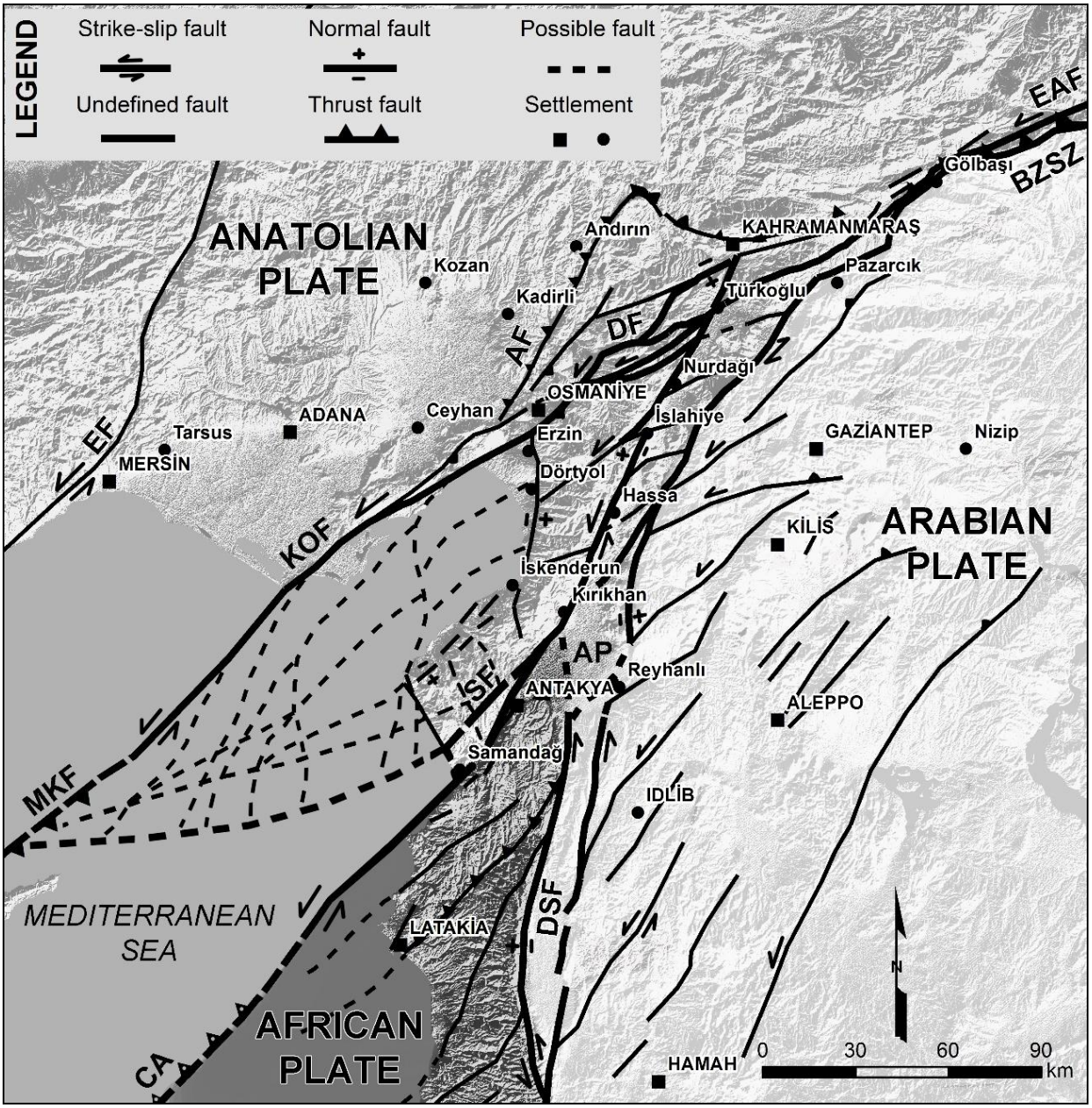

Figure 10: Tectonic model supported by morphometric analyses of alluvial fans (Şengör and Yılmaz, 1981; Günay, 1984; Lyberis et al., 1992; Barka and Reilinger, 1997; Över et al., 2001; Yurtmen et al., 2002; Toprak et al., 2002; Westaway, 2003; Över et al., 2004c; Hardenberg and Robertson, 2007; Boulton and Robertson, 2008; Boulton, 2009, 2013; Karabacak et al., 2010; Emre et al., 2013; Koç and Kaymakçı, 2013; Seyrek et al., 2014; Tarı et al., 2014; Robertson et al., 2015). (**AF:** Aslantaş Fault, **AP:** Amik Plain, **BZSZ:** Bitlis-Zagros Suture Zone, **CA:** Cyprus Arc, **DF:** Deliçay Fault, **DSF:** Dead Sea Fault, **EAF:** East Anatolian Fault, **EF:** Ecemiş Fault, **KOF:** Karataş-Osmaniye Fault, **MKF:** Misis-Kyrenia Fault, **SF:** Samandağ Fault).

This situation corresponds to the view that left lateral slip cannot be compensated with the compression in Bitlis-Zagros suture zone caused by the formation of the Adana-Kilikya in-plate block due to its south to northeast contraction (Şengör and Yılmaz, 1981; Meghraoui et al., 2011).

However, this block is not composed of one piece and is divided into many small blocks. East Anatolian Fault that can be followed up to Türkoğlu in northeast is divided into many branches in this point and cuts Amanos Mountains in northeastern-southwestern direction. From Türkoğlu-Haruniye fault to Deliçay fault, all the faults that diagonally cut Amanos Mountains are branches of East Anatolian Fault (Günay, 1984; Yılmaz, 1984) forming a dispersed plate margin (Figure 10). The border where Anatolian plate completely ends is likely the Cyprus Arc-Hatay Fault

Zonesystem which is the southerly line on which it moves in the south-southwest direction on Mediterranean floor and Misis-Kyrenia Fault Zone which is further west. The Anatolian plate with the southern thrust provided by Eurasian plate drifts towards the Mediterranean. In spite of concave surfaces, including very smooth convex undulations, indicating a transition from divergence regime to convergence regime and sinistral rotational movements of the fans 19, 20 and 21 situated at the northeastern end of the faults which cuts Amanos Mountains diagonally, sharp convex folds containing surfaces, which emphasize an exact convergence regime, and dextral rotational movements of fans 22, 23 and 24 situated at the southwestern end of the same faults are a clear sign of this situation.

Conclusion

Intensive tectonic deformation in the region where Anatolian -part of Eurasian plate-, Arabian and African plates move closest towards each other has made it difficult to accurately determine the plate borders. The relationship between East Anatolian Fault and Dead Sea Fault has turned into a complex one especially in the area called Maraş Triple Junction. Data obtained through morphometric analyses in the zone woven with active faults focusing on alluvial fans were combined with kinematic and geodetic data and crucial clues regarding recent tectonic fault activities in the region. Accordingly, Arabian plate's northern movement is currently met with the thickening of the crust in 150 to 200 km further south along the Bitlis-Zagros suture zone. The first contact, when based on initial speed of the plate 15 mm/year, can be dated to early Upper Miocene for the Northwestern end of the Arabian plate. However, after some time, continuing northern movement of the Arabian plate reached extremely high tension that could not be compensated with crust thickening and the southern part rapidly broke starting from the north of AmikPlain and formed East Anatolian Fault. Sinistral rotational movement of the 24 of 28 fans (two of the others have 2° and two 12° dextral) supports that the tectonic structures are products of the same left lateral dominated mechanism. Anatolian slip to west started at this time and while Bitlis-Zagros Suture Zone was pushed to north and Eurasian southern movement contiued from the north, Anatolian slip continued by collecting the broken parts in the Adana-Kilikya Basin. Such a mechanism resulted in a classic continental plate margin system composed of distributed faults that accomodates deformation over a wide region.

ACKNOWLEDGEMENT

Maps throughout this study were created using ArcGIS® software by Esri. Digital Elevation Model (DEM), which used in this study, ASTER GDEM is a product of METI and NASA.

REFERENCES

Adıyaman Ö, Chorowicz J (2002). Late Cenozoic tectonics and volcanism in the northwestern corner of the Arabian plate: a consequence of the strike-slip Dead Sea fault zone and the lateral escape of Anatolia. J. Volcanol. Geothermal Res. 117: 327–345.

Aksu AE, Calon TJ, Hall J, Yaşar D (2005). Origin and evolution of the Neogene Iskenderun Basin, northeastern Mediterranean Sea. Marine Geology. 22: 161–187.

Albora AM, Sayın N, Uçan OM (2006). Evaluation Of Tectonic Structure Of İskenderun Basin (Turkey) Using Steerable Filters, Marine Geophysical Researches, 27: 225–239.

Allen CR (1969). Active faulting in northern Turkey, Contr. 1577. Div, Geol.Sciences, Calif. Inst. Tech. 32.

Alsdorf D, Barazangi M, Litak R, Seber D, Sawaf T, Al- Saad D (1995). The intraplate Euphrates fault system-Palmyrides mountain belt junction and relationship to Arabian plate tectonics, Annali di Geofisica, XXXVIII, pp. 385–397.

Arger J, Mitchell J, Westaway R (2000). Neogene and Quaternary volcanism of southeastern Turkey, in Tectonics and Magmatism in Turkey and the Surrounding Area, edited by E. Bozkurt, J. A. Winchester, and J. D. A. Piper, Geol. Soc. London Spec. Publ. 173: 459–487.

Arpat E, Şaroğlu F (1973). Türkiye'deki bazı önemli genç tektonik olaylar, TJK Bülteni, 18: 91–101.

Bahrami S (2013). Tectonic controls on the morphometry of alluvial fans around Danehkhoshk anticline, Zagros, Iran. Geomorphology, 180-181: 217–230.

Barka, A. and Reilinger, R.(1997). Active Tectonics of Eastern Mediterranean region: deduced from GPS, neotectonic and seismicity data, Annali di Geofisica, X2(3): 587–610.

Beaty CB (1961). Topographic effects of faulting: Death Valley California. Annals of the Association of American Geographers. 51: 234–240.

Beaumont P (1972). Alluvial fans along the foothills of the Elburz Mountains, Iran: Palaeogeography, Palaeoclimatology, Palaeoecology. 12: 251–273, doi: 10.1016/0031-0182(72)90022-3.

Blair TC, McPherson JG (1994). Alluvial fans and their natural distinction from rivers based on morphology, hydraulic processes, sedimentary processes and facies assemblages. J. Sedimentary Res. A64: 450–489.

Blissenbach E (1954). Geology of alluvial fans in semiarid regions: Geol. Soc. America Bull. 65: 175–189.

Boulton SJ (2009). Record of Cenozoic sedimentation from the Amanos Mountains, Southern Turkey: Implications for the inception and evolution of the Arabia-Eurasia continental collision. Sedimentary Geology. 216: 29–47.

Boulton SJ (2013). Tectonic development of the southern Karasu Valley, Turkey: successive structural events during basin formation. In: Robertson, A. H. F., Parlak, O. and Ünlügenç, U. C. (Eds.), Geological Development of Anatolia and the Easternmost Mediterranean Region. Geological Society of London, Special Publications. 372: 531–546.

Boulton SJ, Robertson AHF (2008). The Neogene–Recent Hatay Graben, South Central Turkey: graben formation in a setting of oblique extension (transtension) related to post-collisional tectonic escape, Geol. Mag. 145(6): 800–821. doi:10.1017/S0016756808005013.

Boulton SJ, Robertson AHF, Unlugenc UC (2006). Tectonic and sedimentary evolution of the Cenozoic Hatay Graben, Southern Turkey: a two-phase model for graben formation. In: Robertson, A. H. F. et al. (eds), Tectonic Development of the Eastern Mediterranean. Special Publication of the Geological Society of London. 260: 613-634.

Boulton SJ, Whittaker AC (2009). Quantifying active faulting in an oblique-extensional graben using geomorphology, drainage patterns and river profiles: Hatay Graben, south central Turkey. Geomorphology. 104: 299-316.

Brink US, Rybakov M, Al-Zoubi AS, Hassouneh M, Frieslander U, Batayneh AT, Goldschmidt V, Daoud MN, Rotstein Y, Hall JK (1999). Anatomy of the Dead Sea transform: Does it reflect continuous changes in plate

motion? Geology. 27(10): 887–890.
Bull W. B. (1964). Geomorphology of segmented Alluvial fans in Western Fresno County, California. Erosion and sedimentation in semiarid environments. US Geological Survey Professional Paper 352-E; 89–129.
Bull WB (1961). Tectonic significance of radial profiles of alluvial fans in Western Fresno County California. US, Geological Survey Professional Paper 424-B. Short Papers in the Geologic and Hydrological Sciences B. 182–184.
Bull WB (1962). Relations of alluvial-fan size and slope to drainage-basin size and lithology in western Fresno County, California: U.S. Geological Survey Professional Paper 424-B, pp. 51–53.
Bull WB (1977). The alluvial fan environment, Progress in Physical Geography. 1: 222–270.
Burbank DW, Anderson RS (2001). Tectonic Geomorphology (Massachusetts: Blackwell Science) pp.274.
Calvache ML, Viseras C, Fernández J (1997). Controls of fan development – evidence from fan morphometry and sedimentology; Sierra Nevada, SE Spain. Geomorphology. 21: 69–84.
Chorowicz J, Luxey P, Lyberis N, Carvalho J, Pairot JF, Yürür T, Gündoğdu N (1994). The Maraş Triple junction (Southern Turkey) based on digital elevation model and satellite imagery interpretation, J.Geophy. Rese. 99(10): 20225–20242.
Courtillot V, Armijo R, Tapponnier P (1987). The Sinai Triple Junction Revisited: Tectonophysics. 141: 181–190.
Çıplak R, ve Akyüz HS (2005). Erkenek-Gölbaşı (Adıyaman) Arasında Doğu Anadolu Fayının Özellikleri. Türkiye Kuvaterner Sempozyumu V, Bildiriler Kitabı, 2-3 Haziran 2005, İTÜ/AYBE.
Demoulin A (1998). Testing the tectonic significance of some parameters of longitudinal river profiles: the case of the Ardenne (Belgium, NW Europe): Geomorphology. 24: 189–208.
Denny CS (1965). Alluvial Fans in the Death Valley Region, California and Nevada, United States Geological Survey, Professional Paper. pp. 466.
Denny CS (1967). Fans and pediments: American J. Sci. 265: 81–105.
Dewey JF, Pindell JL (1985). Neogene block tectonics of eastern Turkey and northern South America: Continental applications of the finite difference method, Tectonics. 4(1): 71–83.
Dewey JF, Pitman WC, Ryan WBF, Bonnin J (1973). Plate tectonics and the evolution of the Alpine System, Geol. Soc. Ame. Bull. 84: 3137–3180.
Dewey JF, Şengör AMC (1979). Aegean and surrounding regions: complex multi-part and continuum tectonics in a convergent zone, Geol. Soc. Ame. Bull. 90: 84–92.
Dilek Y (2010). Eastern Mediterranean geodynamics, International Geology Review. 52: 111–116.
Doornkamp JC, Cuchlaine AMK (1971). Numerical Analysis in Geomorphology. An Introduction. Edward Arnold, London.
Duman TY, Emre Ö (2013). The East Anatolian Fault: Geometry, Segmentation and Jog Characteristics, in: Robertson, A. H. F., Parlak, O. and Ünlügenç, U. C. (Eds.), Geological Development of Anatolia and Easternmost Mediterranean Region. Geological Society,London, Special Publication. 372: 495–529.
Duman TY, Emre Ö, Özalp S, Olgun Ş, Elmacı H (2012). 1/250.000 Scale Active Fault Maps Series of Turkey, Şanlıurfa (NJ 37-10) and Suruç (NJ 37-14) Quadrangles. Serial Number: 43. General Directorate of Mineral Research and Exploration, Ankara-Turkey.
Eagleson PS (1970).DynamicHydrology, McGraw-Hill, New York, USA.
EİE (2005). Göl Gözlemleri. General Directorate of ElectricalPowerResourcesSurveyAnd Development Administration. Ankara-Turkey.
Emre Ö, Duman TY, Olgun Ş (2012a). 1/250.000 Scale Active Fault Maps Series of Turkey, Antakya (NJ 37-13) Quadrangle. Serial Number: 39. General Directorate of Mineral Research and Exploration, Ankara-Turkey.
Emre Ö, Duman TY, Olgun Ş, Elmacı H, Özalp S (2012b). 1/250.000 Scale Active Fault Maps Series of Turkey, Gaziantep (NJ 37-9) Quadrangle. Serial Number: 38. General Directorate of Mineral Research and Exploration, Ankara-Turkey.
Emre Ö, Duman TY, Özalp S, Elmacı H, Olgun Ş, Şaroğlu F (2013). Active Fault Map of Turkey with and Explanatory Text. General Directorate of Mineral Research and Exploration, Special Publication Series-30. Ankara-Turkey.
Erinç S (1973). Türkiyenin şekillenmesinde neotektoniğin rolü ve Jeomorfoloji-Jeodinamik ilişkileri: Jeomorfoloji Dergisi. 5: 15–25.
Erinç S (2000). Jeomorfoloji I. Güncelleştirilmiş 5. Basım, Güncelleştirenler: Ahmet Ertek, Cem Güneysu. Der Yayınları, İstanbul.
Erkmen C, Eravcı B, Özsaraç V, Yaman M, Tekin BM, Albayrak H, Kuterdem K, Aktan T, Tepeuğur E (2009). Doğu Anadolu Fayı'nın Paleosismolojisi Pilot Bölge: "Türkoğlu Gölbası Arası". Türkiye Ulusal Jeodezi ve Jeofizik Birliği (TUJJB) Ulusal Deprem Programı Proje No: TUJJB-UDP-1-07.
Erol O (1983). Newtectonic and geomorphological development of Turkey: Jeomorfoloji Dergisi,. 11: 11–22.
Freund R (1965). A model of the structural development of Israel and adjacent areas since Upper Cretaceous times: Geol. Mag. 102: 189–205.
Garfunkel Z (1981). Internal structure of the Dead Sea leaky transform (rift) in relation to plate kinematics: Tectonophysics. 80: 81–108.
Garfunkel Z, Ben-Avraham Z (1996). The structure of the Dead Sea Basin. Tectonophyics. 266 (1-4): 155–176.
Garfunkel Z, Zak I, Freund R (1981). Active faulting in the Dead Rift: Tectonophysics. 80: 1–26.
Goswami PK, Pant CC, Pandey S (2009). Tectonic controls on the geomorphic evolution of alluvial fans in the Piedmont Zone of Ganga Plain, Uttarakhand, India. J. Earth Syst. Sci. 118: 245–259.
Goudie A (2004). Encyclopedia of Geomorphology. London: Routledge .
Gönençgil B, Karataş A (2012). KuseyrPlatosu'nda (Hatay) Miyosen Sonrası Morfojenetik Süreç-Jeomorfolojik Yapı İlişkisi, Türk Coğrafya Dergisi. 59: 11–26.
Görür N, Oktay FY, Seymen İ, Şengör AMC (1984). Palaeotectonic evolution of Tuzgölü basin complex, Central Turkey, in: Dixon J. E., Robertson A. H. F. (Eds.), The geological evolution of the Eastern Mediterranean, Geological Society Special Publication no. 17, Geological Society, London. pp. 81–96.
Gülen L, Barka A, Toksöz MN (1987). Kıtaların çarpışması ve ilgili kompleks deformasyon, Maraş üçlü eklemi ve çevre yapıları, Yerbilimleri. 14: 319–336.
Günay Y (1984). Amanos Dağları'nın Jeolojisi ve Karasu - Hatay Grabeninin Petrol Olanakları. TPAŞ arama Grubu Başkanlığı Hakkari-Şaryaj Projesi.TPAO Rap. No:1954.
Gürsoy H, Tatar O, Piper JDA, Heimann A, Mesci BL (2003). Neotectonic deformation linking the East Anatolian and Karataş-Osmaniye intracontinental transform fault zones in the Gulf of İskenderun, Southern Turkey, deduced from paleomagnetic study of the Ceyhan-Osmaniye Volcanics. Tectonics. 22(6): 1067–1079.
Gürsoy H, Tatar O, Piper JDA, Koçbulut F, Akpınar Z, Huang B, Roberts AP, Mesci BL (2011). Paleomagnetic study of Kepezdağ and Yamadağ volcanic complexes, central Turkey: Neogene tectonic escape and block definition in the central-east Anatolides. J. Geodynamics. 51: 308–326.
Gvirtzman Z, Steinberg J (2011). Inland Jump of the Arabian Northwest Plate Boundary from the Levant Continental Margin to the Dead Sea Transform. The Mınıstry of Natıonal Infrastructures, Geologıcal Survey of Israel, Fundamental studies for promoting hydrocarbon exploration in Israel Submitted to the Israel Oil Commissioner, Report GSI/29/2011, Jerusalem.
Hack JT (1957). Studies in LongitudinalStreamProfiles in Virginia and Maryland. U.S. GeologicalSurvey Professional Paper. 249: 45–97.
Hack JT (1973). Stream Profile Analysis andStream-Gradient Index. U.S. Geological Survey J. Res. 1: 421–429.
Hall J, Aksu AE, Calon TJ, Yaşar D (2005). Varying tectonic control on basin development at an active microplate margin: Latakia Basin eastern Mediterranean. Marine Geology. 221: 15–60.
Hardenberg MF, Robertson AHF (2007). Sedimentology of the NW margin of the Arabian plate and the SW–NE trending Nahr El-Kabir half-graben in northern Syria during the latest Cretaceous and Cenozoic. Sedimentary Geology. 20: 231–266.
Harvey AM (1987). Alluvial fan dissection: Relationships between morphology and sedimentation, in Frostick, L.E, and Reid, I., eds., Desert sediments: Ancient and modern: Geological Society of London Special Publication. 35: 87–103.
Harvey AM (1990). Factors influencing Quaternary alluvial fan development in southeast Spain. In: RACHOCKI, A.H. & CHURCH, M. (eds) Alluvial Fans: A field Approach. Wiley, Chichester. Pp. 247–269.
Harvey AM (2002). The role of base-level change in the dissection of alluvial fans: case studies from southeast Spain and Nevada. Geomorphology. 45: 67–87.

Harvey AM, Mather AE, Stokes M (2005). Alluvial fans: geomorphology, sedimentology, dynamics - introduction. A review of alluvial-fan research. In: Harvey, A. M., Mather, A. E. and Stokes, M. (eds) Alluvial Fans: Geomorphology, Sedimentology, Dynamics. Geological Society, London, Special Publications. 251: 1–7.

Heimann A, Ron H (1993). Geometric changes of plate boundaries along part of the northern Dead Sea Transform: geochronologic and palaeomagnetic evidence. Tectonics. 12: 477–491.

Herece E (2008). Doğu Anadolu Fayı (DAF) Atlası. Maden Tetkik ve Arama Genel Müdürlüğü, Özel Yayın Serisi 13, Ankara.

Hooke RL (1967). Processes on arid-region alluvial fans. J. Geol. 75: 438–460.

Hooke RLB, Rohrer WL (1979). Geometry of alluvial fans: Effect of discharge and sediment size: Earth Surface Processes and Landforms. 4: 147–166.

Horton RE (1932). Drainage Basin Characteristics. Transaction of American Geological Union. 13: 350–361.

Horton RE (1945). Erosional Development of Streams and Their Drainage Basins: Hydrophysical Approach to Quantitative Morphology. Bulletin of the Geological Society of America. 56: 275–370.

Hoşgören Y (2011). Jeomorfoloji Terimleri Sözlüğü. Çantay Kitabevi, İstanbul.

Joffe S, Garfunkel Z (1987). Plate kinematics of the circum Red Sea- a re-evaluation: Tectonophysics. 141: 5–22.

Kahle HG, Cocard M, Peter Y, Geiger A, Reilinger R, Barka A, Veis G (2000). GPS derived strain rate field within the boundary zones of the Eurasian, African and Arabian Plates, J. Geophys. Res. 105: 23353–23370.

Karabacak V, Akyüz HS, Kıyak NG, Altunel E, Meghraoui M, Yönlü Ö (2012). Doğu Anadolu Fay Zonu'nun Gölbaşı (Adıyaman) ile Karataş (Adana) arasındaki kesiminin geç Kuvaterner aktivitesi, TÜBİTAK Proje No: 109Y04.

Karabacak V, Altunel E, Meghraoui M, ve Akyüz HS (2010). Field Evidences From Northern Dead Sea Fault Zone (South Turkey): New Findings for The Initiation Age and Slip Rate. Tectonophysics. 480: 172–182.

Karataş A, Korkmaz H (2012). Hatay İli'nin Su Potansiyeli ve Sürdürülebilir Yönetimi. I. Baskı, Color Ofset. Mustafa Kemal Üniversitesi, Yayın No: 40.

Karig DE, Kozlu H (1990). Late Palaeogene-Neogene evolution of the triple junction region near Maraş, south-central Turkey, Journal of the Geological Society, London. 147: 1023–1034.

Kearey P, Klepeis KA, Vine FJ (2009). Global Tectonics (3rd Edition), Hoboken, N.J., Wiley-Blackwell.

Kelling G, Gökçen SL, Floyd PA, Gökçen N (1987). Neogene tectonics and plate convergence in the Eastern Mediterranean: new data from southern Turkey, Geology. 15: 425–429.

Kempler D, Garfunkel Z (1991). Northeast Mediterranean triple junction from a plate kinematics point of view, Bulletin of the Technical University of İstanbul, Special Issue. 44: 425–454.

Kempler D, Garfunkel Z (1994). Structures and kinematics in the northeastern Mediterranean: a study of an irregular plate boundary, Tectonophysics. 234: 19– 32.

Ketin İ (1966). Anadolu'nun tektonik birlikleri : MT.Adergisi. 66: 20–34.

Khalifa A, Çakır Z, Owen LA, Kaya Ş (2018). Morphotectonic analysis of the East Anatolian Fault, Turkey. Turkish J. Earth Sci. 27: 110–126.

Kiratzi A (1993). A study on the active crustal deformation of the North and East Anatolian Fault Zones, Tectonophysics. 225: 191–203.

Koç A, Kaymakçı N, Hinsbergen DJJ, Kuiper KF, Vissers RLM (2012). Tectono-Sedimentary evolution and geochronology of the Middle Miocene Altınapa Basin, and implications for the Late Cenozoic uplift history of the Taurides, southern Turkey. Tectonophysics. 532–535: 134–155.

Koç A, Kaymakçı N (2013). Kinematics of Sürgü Fault Zone (Malatya, Turkey): A remote sensing study. J. Geodynamics. 65: 292–307.

Koçbulut F, Akpınar Z, Tatar O, Piper JDA, Roberts AP (2013). Palaeomagnetic study of the Karacadağ Volcanic Complex, SE Turkey: Monitoring Neogene anticlockwise rotation of the Arabian Plate. Tectonophysics. 608: 1007–1024.

Koçyiğit A, Beyhan A (1998). A new intracontinental transcurrent structure: the Central Anatolian Fault Zone, Turkey, Tectonophysics. 284: 317–336.

Krishnamurthy J, Srnivas G, Jayaram V, Chandrasekhar MG (1996). Influence of RockTypesandStructures in the Development of Drainage Networks in TypicalHardrockTerrain. ITC Journal. 3–4: 252–259.

Langbein WB (1964). Profiles of rivers of uniform discharge. United States Geological Survey Professional Paper. 501: 119–122.

Lecce SA (1990). The alluvial fan problem. In Rachocki, A.H. and Church, M., eds. Alluvial Fans: A Field Approach. John Wiley and Sons, Ltd. Pp.391.

Lee J, Spencer J, Owen L (2001). Holocene slip rates along the Owens Valley fault, California: Implications for the recent evolution of the Eastern California Shear Zone. Geology. 29 (9): 819–822.

Leopold LB, Miller JP (1956). EphemeralStreams: HydraulicFactorsandtheirRelationtotheDrainage Network. U.S. GeologicalSurvey, GeologicalSurvey Professional Paper 282 A, Washington, D.C. pp. 1–37.

Leopold LB, Wolman MG, Miller JP (1964). Fluvial Processes in Geomorphology, San Francisco, W.H. Freeman and Co., pp. 522.

Lovelock PER (1984). A review of the tectonics of the northern Middle East region, Geol. Mag. 121 (6): 577–587.

Lyberis N (1988). Tectonic Evolution of the Gulf of Suez and the Gulf of Aqaba. Tectonophysics. (153): 209–221.

Lyberis N, Yürür T, Chorowicz J, Kasapoğlu E, Gündoğdu N (1992). The East Anatolian Fault: An Oblique Collisional Belt, Tectonophysics. 204: 1–15.

Mahadevaswamy G, Nagaraju D, Siddalingamurthy S, Lakshmamma, Mohammad SI, Nagesh PC, Krishna R (2011). Morphometric Analysis of Nanjangud Taluk, Mysore District, Karnataka, India, Using GIS Techniques. Int. J. Geomatics Geosci. 1(4): 721–734.

Mahmoud Y, Masson F, Meghraoui M, Çakır Z, Alchalbi A, Yavaşoğlu H, Yönlü Ö, Daoud M, Ergintav S, İnan S (2013). Kinematic study at the junction of the East Anatolian fault and the Dead Sea fault from GPS measurements. J. Geodynamics. 67: 30–39.

Marchi L, Cavalli M, D'Agostino V (2010). Hydrogeomorphic processes and torrent control works on a large alluvial fan in the eastern Italian Alps. Nat. Hazards Earth Syst. Sci. 10: 547–558.

Marchi L, Pasuto A, Tecca PR (1993). Flow processes on alluvial fans in the Eastern Italian Alps: Zeitschrift fur Geomorphologie. 37(4): 447–458.

McKenzie DP (1970). Plate tectonics of the Mediterranean region, Nature. 220: 239–343.

McKenzie DP (1972). Active tectonics of the Mediterranean region. Geophys. J. R. Astron. Soc. 30: 109–185.

McKenzie DP (1976). The East Anatolian fault: A major structure in eastern Turkey, Earth and Plan. Sci. Lett. 29: 189–193.

Meghraoui M, Çakır Z, Masson F, Mahmood Y, Ergintav S, Alchalbi A, İnan S, Daoud, M, Yönlü Ö, Altunel E (2011). Kinematic modelling at the triple junction between the Anatolian, Arabian, African plates (NW Syria and in SE Turkey). EGU General Assembly 2011, Vienna, Austria.

Melton MA (1957). An Analysis of theRelationsAmongElements of Climate, SurfacePropertiesandGeomorphology. Proj. NR 389-042, Tech. Rep 11, Columbia University, Department of Geology, ONR, New York.

Mills HH (2000). Controls on form, process, and sedimentology of alluvial fans in the Central and Southern Appalachians, southeastern U.S.A: Southeastern Geology. 39: 281–313.

Molin P, Pazzaglia FJ, Dramis F (2004). Geomorphic expression of active tectonics in a rapidly deforming forearc, SilaMassif, Calabria, Southern Italy: American J. Sci. 304: 559–589.

Morisawa ME (1959). Relation of MorphometricPropertiestoRunoff in theLittleMillCreek, Ohio, DrainageBasin. Tech. Rep., 17. Department of Geology, ONR, ColombiaUniversity, New York.

MTA (2002). 1/500.000 Ölçekli Türkiye Jeoloji Haritası. Hatay Paftası.

Muehlberger RW, Gordon MB (1987). Observations on the complexity of the East Anatolian Fault, Turkey, J.Structural Geol. 9: 899–903.

Mueller J (1968). An Introduction to the Hydraulic and Topographic Sinuosity Indexes1. Annals of the Association of American Geographers. 58(2): 371.

Nag SK (1998). Morphometric Analysis Using Remote SensingTechniques in theChakaSub-basin, PuruliaDistrict, West Bengal. J. Indian Soc. Remote Sensing. 26: 1-2.

Nag SK, Chakraborty S (2003). Influence of RockTypesandStructures in The Development of Drainage Network in Hard RockArea. Journal of Indian Society of Remote Sensing. 31: 25–35.

Oguchi T, Kazuaki H, Oguchi CT (2008). Paleohydrologicalimplications of Late Quaternary fluvialdeposits in and around archaeologicalsites in

Syria. Geomorphology 101: 33–43.
Oguchi T, Oguchi CT (2004). LateQuaternaryrapidtalusdissectionanddebrisflowdeposition on an alluvial fan in Syria. Catena. 55: 125–140.
Över S, Kavak KŞ, Bellier O, Özden S (2004a). Is the Amik Basin (SE Turkey) a Triple-JunctionArea? Analyses of SPOT XS Imagery and Seismicity. Int. J. Remote Sensing. 25(19): 3857–3872.
Över S, Özden S, Ünlügenç UC, Yılmaz H (2004c). A synthesis: Late Cenozoic stress field distribution at northeastern corner of the Eastern Mediterranean, SE Turkey, C. R. Geoscience. 336: 93–103.
Över S, Özden S, Ünlügenç UC. (2004d). Late Cenozoic stress distribution along the Misis Range in the Anatolian, Arabian, and African plate intersection region, SE Turkey. Tectonics 23, TC3008.
Över S, Özden S, Yılmaz H (2004b). Late Cenozoic stress evolution along the Karasu Valley, SE Turkey, Tectonophysics. 380: 43–68.
Över S, Ünlügenç UC, Bellier O (2002). Quaternary stress regime change in the Hatay region (SE Turkey). Geophys. J. Int. 148: 1–14.
Över S, Ünlügenç UC, Özden S (2001). Hatay Bölgesinde Etkin Gerilme Durumları. Yerbilimleri. 23: 1–14.
Perinçek D, Çemen İ (1990). The structural relationship between the East Anatolian and Dead Sea fault zones in southeastern Turkey, Tectonophysics: 172: 331–340.
Pinter N, Keller EA (1995a). Quaternary tectonic and topographic evolution of the Northern Owens Valley.In: Hall Jr., C.A., Doyle-Jones, V. and Widawski,B. (Eds.) The History of Water: Eastern Sierra Nevada, Owens Valley, White-Inyo Mountains. White Mt. Research Station, Los Angeles. pp. 32–39.
Pinter N, Keller EA (1995b). Late-Quaternary deformation in northern Owens Valley, California: Geomorphic analysis of tectonic tilt; Geol. Runds. 84: 200–212.
Pope RJJ, Wilkinson KN (2005). Reconciling the roles of climate and tectonics in Late Quaternary fan development on the Spartan piedmont, Greece. Alluvial Fans: Geomorphology, Sedimentology, Dynamics. In: Harvey, A. M., Mather, A. E. and Stokes, M. (eds) Alluvial Fans: Geomorphology, Sedimentology, Dynamics. Geological Society, London, Special Publications. 251: 133–152.
Quennell AM (1956). Tectonics of the Dead Sea rift, Congreso Geologico Internacional, 20th sesion, Asociacion de Servicios Geologicos Africanos: Mexico City, pp. 385–405.
Reilinger R, McClusky S, Vernant P, Lawrence S, Ergintav S, Cakmak R, Ozener H, Kadirov F, Guliev I, Stepanyan R (2006). GPS constraints on continental deformation in the Africa–Arabia–Eurasia continental collision zone and implications for the dynamics of plate interactions. J. Geophy. Res. Pp.111.
Reilinger RE, Mcclusky SC, Oral MB (1997). Global positioning system measurements of present-day crustal movements in the Arabia-Africa-Eurasia plate collision zone. J. Geophy. Res. 102: 9983–9999.
Robertson A, Boulton SJ, Taslı K, Yıldırım N, İnan N, Yıldız A, Parlak O (2015). Late Cretaceous-Miocene sedimentary development of the Arabian continental margin in SE Turkey (Adıyaman Region): implications for regional palaeogeography and the closure history of Southern Neotethys. J. Asian Earth Sci. doi: http://dx.doi.org/10.1016/j.jseaes.2015.01.025.
Robertson AHF, Ünlügenç U, İnan N, Taşlı K (2004). Misis-Andrın Complex: melange formation related to closure and collision of the South-Tethys in S Turkey. J. Asian Earth Sci. 22: 413–453.
Robinson SA, Black S, Sellwood BW, Valdes PJ (2006). A review of palaeoclimates and palaeoenvironments in the Levant and eastern Mediterranean from 25,000 to 5000 years BP: Setting the environmental background for the evolution of human civilisation, Quat. Sci. Rev. 25: 1517–1541. doi:10.1016/j.quascirev.2006.02.006.
Rojay B, Heimann A, Toprak V (2001). Neotectonic and volcanic characteristics of the Karasu fault zone (Anatolia, Turkey): The transition zone between the Dead Sea transform and the East Anatolian fault zone, Geodinamica Acta. 14: 197–212.
Romieh MA, Westaway R, Daoud M, Radwan Y, Yassminh R, Khalil A, Al-Ashkar A, Loughlin S, Arrell K, Bridgland D (2009). Active crustal shortening in NE Syria revealed by deformed terraces of the River Euphrates. Terra Nova. 21(6): 427–437.
Ron H, Freund R, Garfunkel Z, Nur A (1984). Block rotation by strike slip faulting: structural and palaeomagnetic evidence. J. Geophys. Res. 89: 6256–6270.
Rotstein Y (1984). Counterclockwise rotation of the Anatolian block, Tectonophysics. 108: 71–91.
Schumm SA (1956). The Evolution of Drainage Systems and Slopes in Bad Lands at Perth, Amboi, New Jersey. Geol. Soc. Ame. Bull. 67 (5): 597–646.
Seyrek A, Demir T, Pringle M, Yurtmen S, Westaway Reck A, Rowbotham G (2007). Kinematics of the Amanos Fault, southernTurkey, from Ar-Ar dating of offset Pleistocenebasaltflows: transpression between the African and Arabian plates. In: Tectonics of Strike-slip Restraining and Releasing Bends (W.D. Cunningham and P. Mann, eds). Geol. Soc. Lond. Spec. Publ. 290: 255–284.
Seyrek A, Demir T, Westaway R, Guillou H, Scaillet S, White TS, Bridgland DR (2014). TheKinematics of Central-SouthernTurkey and Northwest Syria Revisited. Tectonophysics. 618: 35–66.
Stock JD, Schmidt KM, Miller DM (2008). Controls on Alluvial Fan Long-Profiles. Geological Society of America Bulletin. 120(5-6): 619–640.
Strahler AN (1952). Hypsometric (Area-Altitude) Analysis of ErosionalTopology. GeologicalSociety of America Bulletin. 63 (11): 1117–1142.
Strahler AN (1957). Quantitative Analysis of Watershed Geomorphology. Transactions of the American Geophysical Union. 8 (6): 913–920.
Strahler AN (1964). QuantitativeGeomorphology of DrainageBasinand Channel Networks. In : Handbook of AppliedHydrology (editedbyV.T.Chow), pp. 439–476.
Şengör AMC (1979). The North AnatolianTransformFault: It's Age, OffsetandTectonicSignificance, J. Geol. Soc. London 136: 269–282.
Şengör AMC, Yılmaz Y (1981). Tethyan evolution of Turkey, a plate tectonic approach: Tectonophysics. 75: 181–241.
Şengör AMC, Yılmaz Y (1983). Türkiye'de Tetis'in Evrimi: Levha Tektoniği Açısından Bir Yaklaşım. Türkiye Jeoloji Kurumu, Yerbilimleri Özel Dizisi, No: 1. Ankara.
Şengör AMC, Görür N, Şaroğlu F (1985). Strike-slip faulting and related basin formation in zone of tectonic escape: Turkey as a case study. In:"Strike-slip deformation, basin deformation and sedimentation", Edited by:K.T. Biddle&N. Christie-Blick. Soc.Econ. Paleont. and Min. Spec. Publ. 37: 227–264.
Tarı U, Tüysüz O, Genç ŞC, İmren C, Blackwell BAB, Lom N, Tekeşin Ö, Üsküplü S, Erel L, Altıok S, Beyhan M (2014). The geology and morphology of the Antakya Graben between the Amik Triple Junction and the Cyprus Arc, Geodinamica Acta. 1–29.
Tatar O, Piper JDA, Gürsoy H, Heimann A, Koçbulut F (2004). Neotectonic deformation in the transition zone between the Dead Sea Transform and the East Anatolian Fault Zone, Southern Turkey: A palaeomagnetic study of the Karasu Rift Volcanism. Tectonophysics. 385:17–43.
Toprak, V., Rojay, B. and Heimann, A. (2002). Hatay Grabeninin Neotektonik Evrimi ve Ölü Deniz Fay Kuşağı ile İlişkisi. TÜBİTAK, Proje No: YDABÇAG-391.
Wells SG, Harvey AM (1987). Sedimentologic and geomorphic variations in storm generated alluvial fans, Howgill Fells, northwest England, Geological Society of America Bulletin. 98: 182–198.
Westaway R (1994). Present-day kinematics of the Middle East and Eastern Mediterranean. J.Geophys. Res. 99: 12071–12090.
Westaway R (2003). Kinematics of the Middle East and Eastern Mediterranean updated. Turk. J. Earth Sci. 12: 5–46.
Westaway R (2004). Kinematic consistency between the Dead Sea Fault Zone and the Neogene and Quaternary left-lateral faulting in SE Turkey. Tectonophysics. 391: 203–237.
Westaway R, Demir T, Seyrek A (2008). Interactive comment on "Geometry of the Turkey-Arabia and Africa-Arabia plate boundaries in the latest Miocene to Mid-Pliocene: the role of the Malatya-Ovacık Fault Zone in eastern Turkey" Earth. 3: 27–35.
Yalçın N (1980). Amanosların Litolojik Karakterleri ve Güneydoğu Anadolu'nun Tektonik Evrimindeki Anlamı, Bulletin of the Geological Society of Turkey. 23: 21–30.
Yılmaz H, Over S, Özden S (2006). Kinematics of the East Anatolian Fault Zone between Turkoglu (Kahramanmaras) and Celikhan (Adıyaman), eastern Turkey. Earth, Planets and Space. 58: 1463–1473.
Yılmaz Y (1984). Amanos Dağları'nın Jeolojisi (Cilt: III) Yapı ve Tektonik, T.P.A.O. Rap. No:1920, Ankara.
Yılmaz Y, Gürpınar O, Gül MA, Kozlu H, Yıldırım M, Yiğitbaş E, Genç C,

Keskin M (1985). Maraş Kuzeyinin Jeolojisi (Engizek-Berit-Nurhak-Binboğa-Andırın Dağları), Cilt-1, İstanbul Üniversitesi Mühendislik Fakültesi Döner Sermaye İşletmesi, Rapor No: 2028.

Yönlü Ö, Altunel E, Karabacak V, Akyüz HS (2013). Evolution of the Gölbaş¸ı basin and its implications for the long-term offset on the East Anatolian Fault Zone, Turkey, J. Geodynamics. 65: 272–281.

Yurtmen S, Guillou H, Westaway R, Rowbotham G, Tatar O (2002). Rate of strike-slip motion on the Amanos Fault Karasu Valley, southern Turkey constrained by K-Ar dating and geochemical analysis of Quaternary basalts. Tectonophysics. 344(3-4): 207–246.

Yurtmen S, Rowbotham G, İşler F, Floyd PA (2000). Petrogenesis of basalts from Southern Turkey: The Plio-Quaternary volcanism to the North of İskenderun Gulf. Tectonics and Magmatism in Turkey and the Surrounding Area, Geological Society, London, special Publications. 173: 489–512.

Yürür MT, Chorowicz J (1998). Recent volcanism, tectonics and plate kinematics near the junction of the African, Arabian and Anatolian plates in the Eastern Mediterranean. J. Volcanol. Geothermal Res. 85: 1–15.

Zaprowski B, Pazzaglia FJ, Evenson EB (2005). Climatic influences on profile concavity and river incision: J. Geophy. Res. Earth Surface. 110. Web: http://rasatlar.dsi.gov.tr/

Cite this article as:

Karataş A, Boulton SJ (2019). Morphometric characteristics of alluvial fans in Southern Turkey: implications for fault activity in the Anatolia, Arabia, Africa Triple Junction Region. Acad. J. Environ. Sci. 7(3): 009-029.